OPTIMUM DESIGN OF ANTI-BUCKLING BEHAVIOUR OF THE LAMINATED COMPOSITES CONSIDERING PUCK FAILURE CRITERION BY GENETIC ALGORITHM

A Thesis Submitted to
the Graduate School of Engineering and Sciences of
İzmir Institute of Technology
in Partial Fulfillment of the Requirements for the Degree of

MASTER OF SCIENCE

in Mechanical Engineering

by
Hamza Arda DEVECİ

December 2011
İZMİR

We approve the thesis of **Hamza Arda DEVECİ**

Assist. Prof. Dr. H. Seçil ARTEM
Supervisor

Prof. Dr. Ramazan KARAKUZU
Committee Member

Assoc. Prof. Dr. Alper TAŞDEMİRCİ
Committee Member

19 December 2011

Prof. Dr. Metin TANOĞLU
Head of the Department of
Mechanical Engineering

Prof. Dr. R. Tuğrul SENGER
Dean of the Graduate School
of Engineering and Sciences

ACKNOWLEDGMENTS

I would like to express my sincere gratitude to my supervisor Assist. Prof. Dr. H. Seçil Artem for her advises, guidance, support, encouragement and inspiration through the thesis. Her patience and kindness are greatly appreciated. I have been fortunate to have Dr. Artem as my advisor and I consider it an honor working with her.

I would like to thank also Dr. Levent Aydın for his guidance, support and encouragement, which made my dissertation a better work.

I am also grateful to my friends for their support, encouragement and contributions.

Lastly, I would like to thank my family who have supported and encouraged me during my graduate studies.

ABSTRACT

OPTIMUM DESIGN OF ANTI-BUCKLING BEHAVIOUR OF THE LAMINATED COMPOSITES CONSIDERING PUCK FAILURE CRITERION BY GENETIC ALGORITHM

In recent years, fiber-reinforced composite materials have been increasingly used in engineering applications due to their advantages such as strength and weight reduction. Determination of the buckling load capacity of a composite plate under in-plane compressive loads is crucial for the design of composite structures. Accordingly, in this thesis, optimum designs of anti-buckling behavior of 64-layered carbon/epoxy composite plates, which are simply supported on four sides and subject to biaxial compressive in-plane loads, are investigated considering Puck failure criterion by using genetic algorithm (GA). The plates are taken to be symmetric and balanced with continuous fiber angles in the laminate sequences. Critical buckling load factor is taken as objective function and fiber orientations are taken as design variables. The critical buckling load factor is maximized for various loading cases and plate aspect ratios. The optimum designs obtained are controlled layer by layer using Puck failure criterion. A comparison between continuous and discrete plate (laminate in which the orientation angles are limited to the conventional orientations) designs is performed in order to show the reliability of continuous plates. The optimization of 48-layered composite plates has been performed in order to be compared with 64-layered composite plates. The optimum designs considering Puck inter-fiber failure mode C has also been investigated.

Finally, a comparative study between Puck and Tsai-Wu failure criteria is performed and the advantage of Puck failure criterion is shown. In conclusion, it is found that the optimum designs of laminated composites considering buckling and ply failure strength depend on loading, loading ratio and plate aspect ratio.

ÖZET

TABAKALI KOMPOZİTLERİN BURKULMA KARŞITI DAVRANIŞLARININ PUCK KIRILMA KRİTERİ ESAS ALINARAK GENETİK ALGORİTMA İLE OPTİMUM TASARIMI

Son yıllarda fiber katkılı, tabakalı kompozit malzemeler, dayanıklılık ve ağırlık azaltımı gibi avantajlarına bağlı olarak mühendislik uygulamalarında artan bir şekilde kullanılmaktadır. Düzlem-içi bası yükleri altındaki bir kompozit plakanın burkulma yükü kapasitesinin belirlenmesi kompozit yapıların tasarımı için çok önemlidir. Buna göre, bu tezde, çift eksenli düzlem içi bası yüklere maruz ve dört taraftan basit mesnetli 64 tabakalı karbon/epoksi kompozit plakaların burkulma karşıtı davranışlarının optimum tasarımı Puck kırılma kriteri esas alınarak genetik algoritma (GA) ile araştırılmıştır. Plakalar, levha dizilimlerinde sürekli fiber açılara sahip olacak şekilde simetrik ve balans olarak alınmıştır. Kritik burkulma yükü faktörü amaç fonksiyonu ve fiber oryantasyonları tasarım değişkenleri olarak alınmıştır. Kritik burkulma yükü faktörü çeşitli yükleme durumları ve plaka en-boy oranları için maksimize edilmiştir. Elde edilen optimum tasarımlar Puck kırılma kriterinden yararlanılarak tabaka tabaka kontrol edilmiştir. Sürekli ve belirli plaka (oryantasyon açıları geleneksel oryantasyonlara sınırlanmış levha) tasarımları arasında bir kıyaslama sürekli tasarımların güvenilirliğini göstermek için gerçekleştirilmiştir. 48 tabakalı kompozit plakaların optimizasyonu 64 tabakalı kompozit plakalarla kıyaslanması için sunulmuştur. Optimum tasarımlar, Puck tabakalar arası kırılma C modu dikkate alınarak ayrıca araştırıldı. Son olarak, Puck ve Tsai-Wu kırılma kriterleri arasında bir kıyaslama çalışması gerçekleştirilmiş ve Puck kırılma kriterinin avantajı gösterilmiştir. Sonuç olarak, tabakalandırılmış kompozitlerin burkulma ve lamina kırılma dayanımı dikkate alınarak optimum tasarımlarının yük, yük oranı ve plaka en-boy oranına bağlı olduğu bulunmuştur.

TABLE OF CONTENTS

LIST OF FIGURES viii

LIST OF TABLES ix

CHAPTER 1. INTRODUCTION 1
1.1. Literature Survey 1
1.2. Objectives 5

CHAPTER 2. COMPOSITE MATERIALS 6
2.1. Introduction 6
2.2. Classification of Composites 8
2.2.1. Polymer Matrix Composites 9
2.2.2. Metal Matrix Composites 12
2.2.3. Ceramic Matrix Composites 13
2.2.4. Carbon-Carbon Composites 14
2.3. Applications of Composite Materials 15

CHAPTER 3. MECHANICS OF COMPOSITE MATERIALS 17
3.1. Classical Lamination Theory 17
3.2. Buckling Theory of Laminated Composite Plates 22

CHAPTER 4. FAILURE THEORIES IN COMPOSITE PLATES 24
4.1. Traditional Failure Theories 24
4.1.1. Maximum Stress Theory 24
4.1.2. Tsai-Wu Failure Criterion 25
4.2. Puck Failure Criterion (PFC) 26
4.2.1. Puck Fiber Failure (FF) 26
4.2.2. Puck Inter-Fiber Failure (IFF) 27

CHAPTER 5. OPTIMIZATION 31
5.1. Introduction 31

5.2. Definition of Optimization Problem 33
5.3. Genetic Algorithm (GA) 34
5.3.1. Terminology 35
5.3.2. Breeding 36
5.3.2.1. Selection 37
5.3.2.2. Crossover (Recombination) 37
5.3.2.3. Mutation 38
5.3.2.4. Replacement 38
5.4. MATLAB Optimization Toolbox 39
5.4.1. Genetic Algorithm Solver (ga) 39

CHAPTER 6. RESULTS AND DISCUSSION 43
6.1. Problem Definition 43
6.2. Optimization Results and Evaluation 45

CHAPTER 7. CONCLUSION 69

REFERENCES 71

APPENDIX A. MATLAB COMPUTER PROGRAM 74

LIST OF FIGURES

Figure **Page**

Figure 2.1. Specific strength as a function of time of use of materials 7
Figure 2.2. Types of composites based on reinforcement shape 8
Figure 2.3. Comparison of performance of several common matrices used in polymer matrix composites 11
Figure 2.4. Stealth aircraft 16
Figure 2.5. Use of fiber-reinforced polymer composites in Airbus 380 16
Figure 3.1. A thin fiber-reinforced laminated composite subjected to in plane loading 18
Figure 3.2. Coordinate locations of plies in a laminate 18
Figure 3.3. Resultant forces and moments on a laminate 20
Figure 4.1. Principal material coordinates of a typical lamina 27
Figure 4.2. Three-dimensional stresses on a UD composite element. (x_1, x_2, x_3) coordinate system is fixed to fiber direction (x_1), laminate mid-surface (x_2) and thickness direction (x_3). The (x_1, x_n, x_t) coordinate system is rotated by an angle θ_{fp} from the x_2 direction to the x_n direction which is normal to the fracture plane. The inter-fiber fracture is influenced by the the three stresses σ_n, τ_{nt}, τ_{n1} only 28
Figure 4.3. (σ_1, τ_{21}) fracture curve for σ_1, representing the three different fracture modes (A, B and C) for the PFC 28
Figure 5.1. Minimum and maximum of objective function (f(x)) 32
Figure 5.2. Flowchart of genetic algorithm 35
Figure 5.3. Representation of a chromosome 36
Figure 5.4. Representation of genes in a chromosome 36
Figure 5.5. Selection process 37
Figure 5.6. Crossover 38
Figure 5.7. Matlab optimization toolbox ga solver user interface 40
Figure 6.1. Laminated composite subjected to in plane loads 43
Figure 6.2. The best and mean values of the objective functions at each generation in GA for (a) $N_x/N_y = 1/2$, (b) $N_x/N_y = 1$, (c) $N_x/N_y = 2$, (d) $N_x/N_y = 4$ 68

LIST OF TABLES

Table **Page**

Table 2.1. Specific Modulus and Specific Strength of Typical Fibers, Composites, and Bulk Metals 8
Table 2.2. Differences between thermosets and thermoplastics 12
Table 2.3. Typical Mechanical Properties of Metal Matrix Composites 13
Table 2.4. Typical Mechanical Properties of Some Ceramic Matrix Composites....14
Table 2.5. Typical Mechanical Properties of Carbon-Carbon Matrix Composites 15
Table 5.1. Methods of Operations Research 32
Table 5.2. Genetic Algorithm parameters used in model problems....42
Table 6.1. The elastic properties of carbon/epoxy layers 44
Table 6.2. Strength properties of the lamina....44
Table 6.3. Verification of objective function algorithm....46
Table 6.4. Verification of Puck failure criterion algorithm....47
Table 6.5. Optimum designs and corresponding failure efforts for $a/b = 1$ 48
Table 6.6. Optimum designs and corresponding failure efforts for $a/b = 2$ 49
Table 6.7. Optimum designs and corresponding failure efforts for $a/b = 4$ 51
Table 6.8. Optimum designs and corresponding failure efforts for $a/b = 1/2$ 52
Table 6.9. Optimum designs and corresponding failure efforts for $N_x = 1000$ N/mm 54
Table 6.10. Optimum designs and corresponding failure efforts for $N_x = 3000$ N/mm 55
Table 6.11. Optimum designs and corresponding failure efforts for $N_x = 5000$ N/mm....56
Table 6.12. Optimum designs and corresponding failure efforts for $N_x = 10000$ N/mm 57
Table 6.13. Comparison of continuous (Cont) and discrete (Disc) optimum designs for $a/b = 2$....59
Table 6.14. Comparison of continuous and discrete optimum designs for $a/b = 1/2$ 61
Table 6.15. Optimum designs of 48-layered plates for $N_x = 3000$ N/mm 62
Table 6.16. Comparison of Puck and Tsai-Wu failure theories for specific designs....63

Table 6.17. All optimum designs of anti-buckling behavior 64
Table 6.18. Inter-fiber failure efforts of optimum designs at N_x = 3000 N/mm loading for mode B ($f_{E(IFFB)}$) and mode C ($f_{E(IFFC)}$) 66

CHAPTER 1

INTRODUCTION

1.1. Literature Survey

Fiber reinforced composites are increasingly used in several modern engineering fields such as aircrafts, aerospace, automotive, and marine due to their low weight, high strength and/or stiffness and better mechanical properties than other materials. Some examples of their applications are lightweight, strong and rigid aircraft frames, composite drive shafts and suspension components, sports equipment, pressure vessels and high-speed flywheels with developed energy storage capabilities. The anisotropic nature of fiber-reinforced composites enables the unique opportunity of tailoring such properties as the stacking sequence, fiber orientation and thickness of laminate according to design requirements for a given application. Consequently, the design of laminated composite materials may be optimized over various objective functions and design variables (Pelletier and Vel 2006).

Many researches have carried out many studies using several optimization techniques according to various optimization objectives in the literature for the optimization of laminated composite materials. The stochastic optimization methods used mostly in the literature are genetic algorithm (GA), simulated annealing algorithm, tabu search, pattern search and ant colony optimization. Furthermore, problems are considered using single-objective or multi-objective approaches in the optimization of laminated composite materials.

Weight or thickness minimization of the laminated composite plates is one of the design objectives used by researchers. The use of a genetic algorithm for the minimum thickness design of composite laminated plates is explored by some pioneers. A previously developed genetic algorithm for laminate design has been revised and improved. Thus, the thinnest symmetric and balanced laminates satisfying the 4-ply contiguity constraint which do not fail because of the fact that buckling or excessive strains are obtained (Le Riche and Haftka 1995). Minimum weight design of composite laminates is presented using genetic algorithm considering the failure mechanism based

(FMB), maximum stress and Tsai-Wu failure criteria as design constraints for different in-plane loading conditions and different ply orientations, which are defined as the design variable (Naik, et al. 2008).

Some researchers have included the minimum weight design to minimum deflection or minimum cost design objectives. The minimum deflection and weight designs of laminated composite plates with four layers considering various boundary conditions, varying aspect ratios and different loading types are given separately using the finite element method based on Mindlin plate theory in conjunction with optimization routines (Walker, et al. 1997). A similar study, a technique for combining genetic algorithms with the finite element method to minimize both the mass and deflection of eight layered symmetric-balanced fiber-reinforced composite plates with fiber orientation and laminate thickness design variables is described considering implemented design constraint based on the Tsai-Wu failure criterion (Walker and Smith 2003). The minimum weight and the minimum material cost of laminated plates subjected to in-plane loads are investigated by genetic algorithm. Maximum stress, Tsai-Wu (TW) and the Puck failure criterion (PFC) are taken into account by means of constraints introduced in the optimization problem. The design variables are the ply orientations, the number of layers and the layer material as usual (Lopez, et al. 2009).

Another optimization method commonly used in composite design is direct search simulated annealing (DSA), which is also a reliable global search algorithm. Minimum thickness (weight) optimization of laminated composite plates having fiber orientation angles and layer thickness as design variables subject to different in-plane loadings has been presented by Akbulut and Sonmez (2008). In their study, the Tsai-Wu and the maximum stress criteria have been used in order to check static failure. The same research team has recently made a similar study thereby improving a new variant of simulated annealing (Akbulut and Sonmez 2011).

The buckling load capacity of a composite plate under in-plane compressive loads is crucial for the design of the composite structures. The buckling could cause a premature failure of the structure. Therefore, buckling load maximization is a critical issue that many researchers deal with. The stacking sequence design of a composite laminate for buckling load maximization considering strain failure has been studied using genetic algorithm by Haftka and Le Riche (1993). Optimum stacking sequence designs of a composite panel subjected to biaxial in-plane compressive loads have been found using genetic algorithm and generalized pattern search algorithm. The critical

buckling loads are maximized for several combinations of load case and plate aspect ratio, and are compared with published results in their study (Soykasap and Karakaya 2007; Karakaya and Soykasap 2009). Similarly, another optimization study using a genetic algorithm is proposed to determine the optimal stacking sequence of laminated composite plates for the maximum buckling load under several different loadings, such as uniaxial compression, shear, biaxial compression, and the combination of shear and biaxial loadings. Critical buckling load is taken as fitness function and fiber orientations are taken as design variables (Kim and Lee 2005).

Some researchers have revised and improved genetic algorithms for searching the optimum designs of composite plates and obtaining more reliable results. Buckling load maximization of a simply supported laminated composite plate by applying genetic algorithm with generalized elitist selection has been examined to obtain optimal designs for symmetric-balanced, simply supported plate assumptions (Soremekun, et al. 2001). Permutation genetic algorithms optimizing the stacking sequence of a composite laminate for maximum buckling load and a comparison with standard non-permutation GA have been presented by Liu et al. (2000).

As in weight minimization design problems, buckling load maximization designs have also handled with another various optimization methods in the literature. An improved version of simulated annealing algorithm, which is direct simulated annealing (DSA), has been utilized to maximize the buckling load capacity of laminated composites subject to given in-plane static loads for critical buckling failure in order to find the optimum fiber orientation by Erdal and Sonmez (2005). Optimum designs of the stacking sequence of a composite laminate for buckling response, matrix cracking and strength requirements have been conducted using a heuristic search technique known as tabu search and compared to the related previous studies done by genetic algorithm (Pai, et al. 2003). An application of the ant colony optimization (ACO) metaheuristic to the stacking sequence design of laminated composite panels for maximization of buckling load with strength constraints is fulfilled and compared to other researches previously studied by using genetic algorithms (GA) and tabu search (TS) to indicate the computational efficiency and the quality of results provided by ACO algorithm (Aymerich and Serra 2008). The Ant Colony Optimization algorithm has been also used with strength constraints to find the optimum designs of composite plates in the literature. For instance, the problem has been formulated to maximize the critical buckling load whereas with the biaxial tension, the formulation is to minimize

the failure index in the study of Sebaey et al. (2011). The modified feasible direction (MFD) method has been used for optimization of symmetrically angle-ply square laminated plates in which the design objective is the maximization of the buckling load for weighted sum of the biaxial compressive and thermal loads. The effect of different weighting factors, number of layers, aspect ratios, load ratios and boundary conditions on the optimal design has been investigated (Topal and Uzman 2010). A Pareto-based multi-objective evolutionary algorithm method is applied to the optimal design of a composite plate for weight minimization and maximization of the buckling margins under three hundred load cases (Irisarri, et al. 2009). Optimal design of composite laminates under buckling load uncertainty is studied and the buckling load is maximized under worst case in-plane loading using a nested solution method. Results are given for both continuous and discrete fiber orientations using a nested solution method (Adali, et al. 2003).

Besides buckling load optimization of composite plates subjected to mechanical loading only, thermal buckling optimization of composite laminates subjected to a thermal change has been investigated in the literature. Thermal buckling optimization problem of laminated composite plates in aerospace structures, which require such components that are able to withstand the external environment loads without loss of stability, subject to a temperature rise is solved under strain and ply contiguity constraints using evolution strategies, a guided random-search method by (Spallino and Thierauf 2000). In another study, thermal buckling optimization of laminated plates subjected to uniformly distributed temperature load is investigated in order to obtain optimum fiber orientation designs having the maximum critical temperature capacity of laminated plates using Modified Feasible Direction (MFD) method (Topal and Uzman 2008).

1.2. Objectives

Considering the literature survey, it is clearly obvious that design criteria includes performance of the panel, material failure, weight, rigidity etc. so that the number of plies (thickness) and stacking sequence can be optimized for a better design. In the same manner, determination of the buckling load capacity of a laminated composite plate under in-plane compressive loads has a critical importance in the design of the composite structures. The buckling could yield a premature failure of the structure. Accordingly, the aims of the thesis can be listed as follows

1) To find the best stacking sequences (fiber orientations with continuous fiber angles) of 64-layered carbon/epoxy laminated composites in different plate aspect ratios subjected to various compressive in-plane loads resisting to buckling and failure of any layer (the first ply failure).
2) Determination and comparison of objective function (buckling load factor) values of optimized composite plates for each design cases.
3) Determination and comparison of effective failure values (f_E) of optimized composite plates for each design case using Puck Failure Criterion.
4) Determination of some discrete fiber orientation designs transforming from continuous and comparison of both discrete and continuous fiber orientations of composite plates in order to show the advantages of the designs having continuous fiber orientation.
5) To obtain the best designs of 48-layered carbon/epoxy composite plates subjected to specific compressive in-plane loading and comparison with the corresponding 64-layered plates in terms of buckling and failure strength.
6) To check reliability of the designs according to Tsai-Wu failure theory commonly used in industry and to show the advantages of Puck failure theory as compared with Tsai-Wu.

CHAPTER 2

COMPOSITE MATERIALS

2.1. Introduction

In general terms, a composite is a structural material that comprises of two or more components that are combined at macroscopic level and are not soluble in each other. One of the components is called the reinforcement and the other one in which it is embedded is called the matrix. The reinforcement material may be in the form of fibers, particles, or flakes. The matrix materials are usually in continuous nature. Concrete reinforced with steel and epoxy reinforced with glass fibers, etc. are some of the examples of composite systems (Kaw 2006).

The combining of materials to create a new material system with improved material properties has been continually practiced in history. For instance, the ancient Egyptian workers during the construction of pyramids included chopped straw in bricks by means of improving their structural integrity. The Japanese Samurai warriors used laminated metals in the forging of their swords to provide desirable material properties. More recently, in the 20^{th} century civil engineers put construction iron into cement and produced a well-known composite material, i.e., reinforced concrete. It can be said that the modern times of composite materials began with fiberglass polymer matrix composites during World War II (Vinson and Sierakowski 2004).

Many fiber-reinforced materials enable a better combination of strength and modulus as compared with many traditional metallic materials. Due to their low density, high strength-weight and modulus-weight ratios, these composite materials are significantly superior to those of metallic materials. Furthermore, fatigue strength as well as fatigue damage tolerance of many laminated composites are pretty good. Therefore, fiber reinforced materials have come up as a major class of structural materials and they are considered for use as substitution for metals in many weight-critical components in aerospace, automotive, and other industries (Mallick 2007).

Figure 2.1 shows the comparison of composites and fibers with the other traditional materials in terms of specific strength on yearly basis.

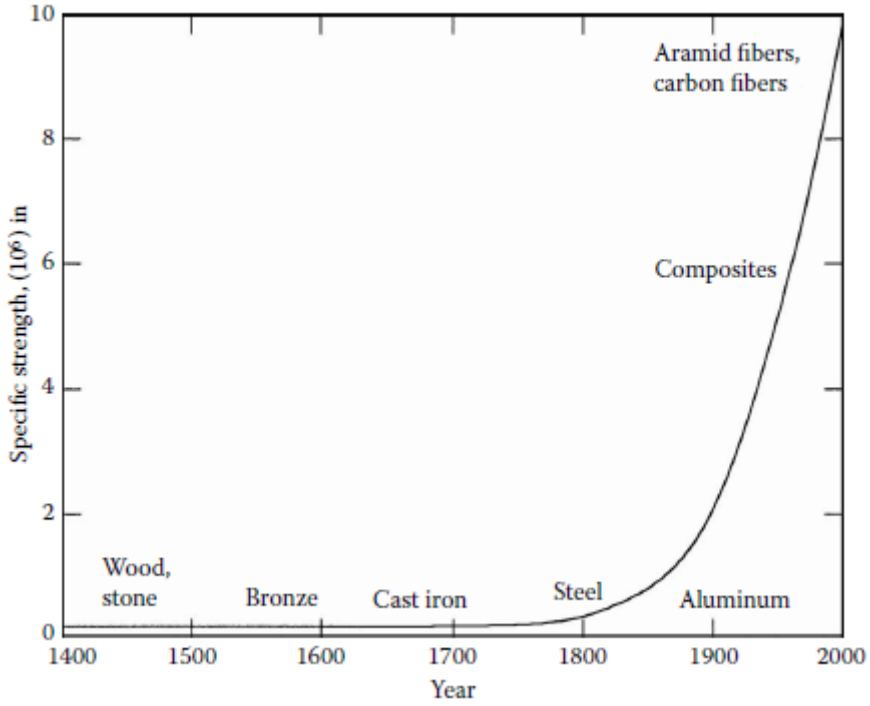

Figure 2.1. Specific strength as a function of time of use of materials
(Source: Kaw 2006)

Specific modulus and specific strength properties for commonly used composite fibers, unidirectional composites, cross-ply and quasi-isotropic laminated composites and monolithic metals are given in Table 2.1 (Kaw 2006).

Table 2.1. Specific Modulus and Specific Strength of Typical Fibers, Composites, and Bulk Metals (Source: Kaw 2006)

Material Units	Specific gravity	Young's modulus (GPa)	Ultimate strength (MPa)	Specific modulus (GPa-m³/kg)	Specific strength (MPa-m³/kg)
System of Units: SI					
Graphite fiber	1.8	230.00	2067	0.1278	1.148
Aramid fiber	1.4	124.00	1379	0.08857	0.9850
Glass fiber	2.5	85.00	1550	0.0340	0.6200
Unidirectional graphite/epoxy	1.6	181.00	1500	0.1131	0.9377
Unidirectional glass/epoxy	1.8	38.60	1062	0.02144	0.5900
Cross-ply graphite/epoxy	1.6	95.98	373.0	0.06000	0.2331
Cross-ply glass/epoxy	1.8	23.58	88.25	0.01310	0.0490
Quasi-isotropic graphite/epoxy	1.6	69.64	276.48	0.04353	0.1728
Quasi-isotropic glass/epoxy	1.8	18.96	73.08	0.01053	0.0406
Steel	7.8	206.84	648.1	0.02652	0.08309
Aluminum	2.6	68.95	275.8	0.02652	0.1061

2.2. Classification of Composites

Composites can be classified by the geometry of the reinforcement such as particulate, flake, and fibers (Figure 2.2) or by the type of matrix such as polymer, metal, ceramic and carbon.

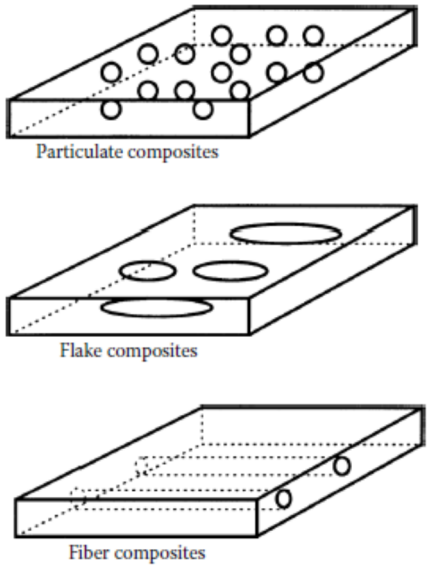

Figure 2.2. Types of composites based on reinforcement shape (Source: Kaw 2006)

Particulate composites include particles embedded in matrices such as alloys and ceramics. The use of aluminum particles in rubber; silicon carbide particles in aluminum; and gravel, sand and cement to make concrete are common examples of particulate composites. Flake composites contain flat reinforcements in matrices. Typical flakes are glass, mica, aluminum, and silver. Fiber reinforced composite materials consist of matrices reinforced by short (discontinuous) or long (continuous) fibers. Fibers are usually anisotropic; carbon, glass and aramids are the most used examples of fibers. Matrices include resins such as epoxy, metals such as aluminum, and ceramics such as calcium-alumina silicate. Continuous fiber matrix composites consist of unidirectional or woven fiber laminas. Laminas are stacked on top of each other at various angles to form a multidirectional laminate (Kaw 2006).

Another type of composite material is the nanocomposites with a big potential of becoming an important material in the future. Although nanocomposites are in the early stages of development, they now attract considerable attention of academia as much as a wide range of industries, including aerospace, automotive, and biomedical industries. The reinforcement in nanocomposites is ensured by either nanoparticles, nanofibers, or carbon nanotubes (Mallick 2007).

2.2.1. Polymer Matrix Composites

Common advanced composites are polymer matrix composites (PMCs) consisting of a polymer such as epoxy, polyester and urethane, reinforced by thin diameter fibers such as graphite, aramids and boron. PMCs are mostly preferred due to their low cost, high strength, and simple manufacturing principles. Some disadvantages of PMCs are low operating temperatures, high coefficients of thermal and moisture expansion and low elastic properties in certain directions.

The most common fibers used are glass, graphite, and Kevlar. Glass is the most common fiber used in polymer matrix composites. Its advantages are its high strength, low cost, high chemical resistance and good insulating properties. The disadvantages are low elastic modulus, poor adhesion to polymers, high specific gravity, sensitivity to abrasion (reduces tensile strength) and low fatigue strength. The main types of glass fibers are E-glass (fiberglass) and S-glass. The “E” in E-glass corresponds to electrical since it was designed for electrical applications. Besides, it is used for many other

purposes now, such as decoration and structural applications. The “S” in S-glass corresponds to higher content of silica. S-glass fibers hold their strength at high temperatures compared to E-glass and have higher fatigue strength. They are used principally for aerospace applications. Other types available commercially are C-glass (Corrosion) used in chemical environments, such as storage tanks; R-glass used in structural applications such as construction; D-glass (Dielectric) used for applications requiring low dielectric constants, such as radomes; and A-glass (Appearance) used to improve surface appearance. Some combinational types such as E-CR glass (Electrical and Corrosion resistance) and AR glass (Alkali Resistant) also exist.

Graphite fibers are more often used in high-modulus and high-strength applications such as aircraft components, etc. The advantages of graphite fibers are high specific strength and modulus, low coefficient of thermal expansion, and high fatigue strength. The disadvantages are high cost, low impact resistance, and high electrical conductivity.

An aramid fiber is an aromatic organic compound made of carbon, hydrogen, oxygen, and nitrogen. The advantages of using aramid fiber are low density, high tensile strength, low cost, and high impact resistance. Its disadvantages are low compressive properties and degradation in sunlight. Kevlar 29® and Kevlar 49® are the two main types of aramid fibers. Both types of Kevlar fibers have similar specific strengths, but Kevlar 49 has a higher specific stiffness. Kevlar 29 is principally used in bulletproof vests, ropes, and cables. Kevlar 49 is used in high performance applications by the aircraft industry.

Various polymers are used in advanced polymer composites. These polymers are such as epoxy, phenolics, acrylic, urethane, and polyamide and each polymer holds its advantages and disadvantages in its use.

Besides, each of the resin systems has its some advantages and disadvantages. The use of a particular resin system depends on the application. These considerations involve mechanical strength, cost, smoke emission, temperature excursions, etc. The comparison of five common resins based on smoke emission, strength, service temperature, and cost is given in Figure 2.3.

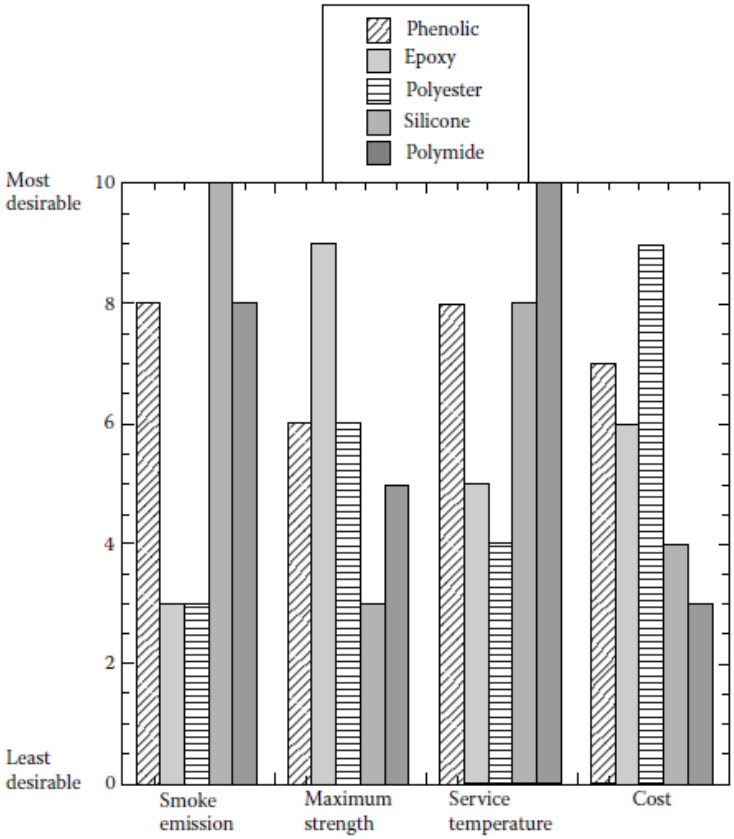

Figure 2.3. Comparison of performance of several common matrices used in polymer matrix composites (Source: Kaw 2006)

Epoxy resins are the most preferred resins. They are low molecular weight organic liquids containing epoxide groups. Epoxide comprises of three members in its molecule ring: one oxygen and two carbon atoms. Epoxy is the most commonly used PMC matrix, however it is costlier than other polymer matrices. More than two-thirds of the polymer matrices used in aerospace applications is epoxy based. Because of their some advantages such as high strength, low viscosity and low flow rates, which allow good wetting of fibers and prevent misalignment of fibers during processing, low volatility during cure, low shrink rates, which reduce the tendency of gaining large shear stresses of the bond between epoxy and its reinforcement, epoxy resins are the most widely held PMC matrix and existing in more than 20 grades to meet specific property and processing requirements.

Polymers are categorized as thermosets and thermoplastics. Thermoset polymers are insoluble and infusible after cure because its molecular chains are rigidly joined with strong covalent bonds; thermoplastics are formable at high pressure and high

temperatures because their molecular bonds are weak and of the van der Waals type. Typical examples of thermosets are epoxies, polyesters, phenolics, and polyamide; typical examples of thermoplastics are polyethylene, polystyrene, polyether–ether–ketone (PEEK), and polyphenylene sulfide (PPS). The differences between thermosets and thermoplastics are indicated in Table 2.2 (Kaw 2006).

Table 2.2. Differences between thermosets and thermoplastics
(Source: Kaw 2006)

Thermoplastics	Thermoset
Soften on heating and pressure, and thus easy to repair	Decompose on heating
High strains to failure	Low strains to failure
Indefinite shelf life	Definite shelf life
Can be reprocessed	Cannot be reprocessed
Not tacky and easy to handle	Tacky
Short cure cycles	Long cure cycles
Higher fabrication temperature and viscosities have made it difficult to process	Lower fabrication temperature
Excellent solvent resistance	Fair solvent resistance

2.2.2. Metal Matrix Composites

Metal matrix composites (MMCs), as the name refers, have a metal matrix. Examples of metal matrices in such composites are aluminum, magnesium, and titanium. Typical fibers used in MMCs are carbon and silicon carbide. Metals are chiefly reinforced to increase or decrease their properties to provide the needs of design. For instance, the stiffness and strength of metals can be increased and large coefficients of thermal expansion and thermal and electric conductivities of metals can be reduced, by the addition of fibers such as silicon carbide.

Metal matrix composites are principally used to get more advantageous than monolithic metals such as steel and aluminum. The advantages of MMCs can be counted as higher specific strength and modulus by reinforcing low-density metals, such as aluminum and titanium; lower coefficients of thermal expansion by reinforcing with fibers with low coefficients of thermal expansion, such as graphite; and maintaining properties such as strength at high temperatures. Metal matric composites have several superiorities in comparison to polymer matrix composites. These advantages are better elastic properties; higher service temperature; insensitivity to moisture; higher electric and thermal conductivities; and better wear, fatigue, and flaw resistances. The

disadvantages of MMCs over PMCs are higher processing temperatures and higher densities. Typical mechanical properties of MMCs are shown in Table 2.3 (Kaw 2006).

Table 2.3. Typical Mechanical Properties of Metal Matrix Composites
(Source: Kaw 2006)

Property	Units	SiC/ aluminum	Graphite/ aluminum	Steel	Aluminum
System of units: USCS					
Specific gravity	—	2.6	2.2	7.8	2.6
Young's modulus	Msi	17	18	30	10
Ultimate tensile strength	ksi	175	65	94	34
Coefficient of thermal expansion	µin./in./°F	6.9	10	6.5	12.8
System of units: SI					
Specific gravity	—	2.6	2.2	7.8	2.6
Young's modulus	GPa	117.2	124.1	206.8	68.95
Ultimate tensile strength	MPa	1206	448.2	648.1	234.40
Coefficient of thermal expansion	µm/m/°C	12.4	18	11.7	23

2.2.3. Ceramic Matrix Composites

Ceramic matrix composites (CMCs) contain ceramic matrix such as alumina calcium alumina silicate reinforced by fibers such as carbon or silicon carbide. The main advantages of CMCs are high strength, hardness, high service temperature limits for ceramics, chemical inertness, and low density. On the other hand, ceramics by themselves have low fracture toughness. Ceramics fail disastrously under tensile or impact loading. The fracture strength of ceramics increases by reinforcing ceramics with fibers, such as silicon carbide or carbon thereby the failure of the composite occurs gradually. The combination of fiber and ceramic matrix makes CMCs more attractive for applications in which high mechanical properties and extreme service temperatures are desired. In Table 2.4, typical mechanical properties of ceramic matrix composites are presented (Kaw 2006).

Table 2.4. Typical Mechanical Properties of Some Ceramic Matrix Composites (Source: Kaw 2006)

Property	Units	SiC/LAS	SiC/CAS	Steel	Aluminum
System of units: USCS					
Specific gravity	—	2.1	2.5	7.8	2.6
Young's modulus	Msi	13	17.55	30.0	10.0
Ultimate tensile strength	ksi	72	58.0	94.0	34.0
Coefficient of thermal expansion	µin./in./°F	2	2.5	6.5	12.8
System of units: SI					
Specific gravity	—	2.1	2.5	7.8	2.6
Young's modulus	GPa	89.63	121	206.8	68.95
Ultimate tensile strength	MPa	496.4	400	648.1	234.4
Coefficient of thermal expansion	µm/m/°C	3.6	4.5	11.7	23

2.2.4. Carbon-Carbon Composites

Carbon–carbon composite (C/C) is a material consisting of carbon fiber reinforcement in a matrix of graphite. Carbon fibers are used in a carbon matrix such as graphite to create carbon-carbon composites. This type of composites can be used in very high-temperature environments of up to 3315°C, and are 20 times stronger and 30% lighter than graphite fibers. Carbon is inherently brittle and flaw sensitive like ceramics. Reinforcement of carbon matrix allows the composite to fail gradually and also ensures some better properties such as ability to withstand high temperatures, low creep at high temperatures, low density, good tensile and compressive strengths, high fatigue resistance, high thermal conductivity, and high coefficient of friction. Main disadvantages of C/C composites are their high cost, low shear strength, and susceptibility to oxidations at high temperatures. Typical properties of carbon–carbon composites are given as comparative with some metals in Table 2.5 below (Kaw 2006).

Table 2.5. Typical Mechanical Properties of Carbon–Carbon Matrix Composites (Source: Kaw 2006)

Property	Units	C–C	Steel	Aluminum
System of units: USCS				
Specific gravity	—	1.68	7.8	2.6
Young's modulus	Msi	1.95	30	10
Ultimate tensile strength	ksi	5.180	94	40
Coefficient of thermal expansion	μin./in./°F	1.11	6.5	12.8
System of units: SI				
Specific gravity	—	1.68	7.8	2.6
Young's modulus	GPa	13.5	206.8	68.95
Ultimate strength	MPa	35.7	648.1	234.4
Coefficient of thermal expansion	μm/m/°C	2.0	11.7	23

2.3. Applications of Composite Materials

There are so various commercial and industrial applications of fiber-reinforced polymer composites so that it is impossible to list them all. In this section, the major structural application areas such as aircraft, space, automotive, sporting goods, marine, and infrastructure are highlighted. Besides these common application fields, fiber-reinforced polymer composites are also used in electronics (e.g., printed circuit boards), building construction (e.g., floor beams), furniture (e.g., chair springs), power industry (e.g., transformer housing), oil industry (e.g., offshore oil platforms and oil sucker rods used in lifting underground oil), medical industry (e.g., bone plates for fracture fixation, implants, and prosthetics), and in many industrial products such as step ladders, oxygen tanks, and power transmission shafts. Potential use of fiber-reinforced composites can be seen in many engineering fields today. A careful design practice and appropriate process development based on the understanding of their unique mechanical, physical, and thermal characteristics are required to put them to actual use.

The main structural applications for fiber-reinforced composites are in the field of military and commercial aircrafts, for which weight reduction is critical for higher speeds and increased loads. The use of fiber-reinforced polymers has experienced a steady growth in the aircraft industry since the production application of boron fiber - reinforced epoxy skins for F-14 horizontal stabilizers in 1969. Carbon fibers are

introduced to industry in the 1970s and carbon fiber-reinforced epoxy has become the indispensable material in many wing, fuselage, and empennage components.

For instance, the outer skin of B-2 (Figure 2.4) and other stealth aircrafts is almost all made of carbon fiber-reinforced polymers. Figure 2.5 schematically illustrates the composite usage in Airbus A380 introduced in 2006. About 25% of its weight is made of composites (Mallick 2007).

Figure 2.4. Stealth aircraft
(Source: Mallick 2007)

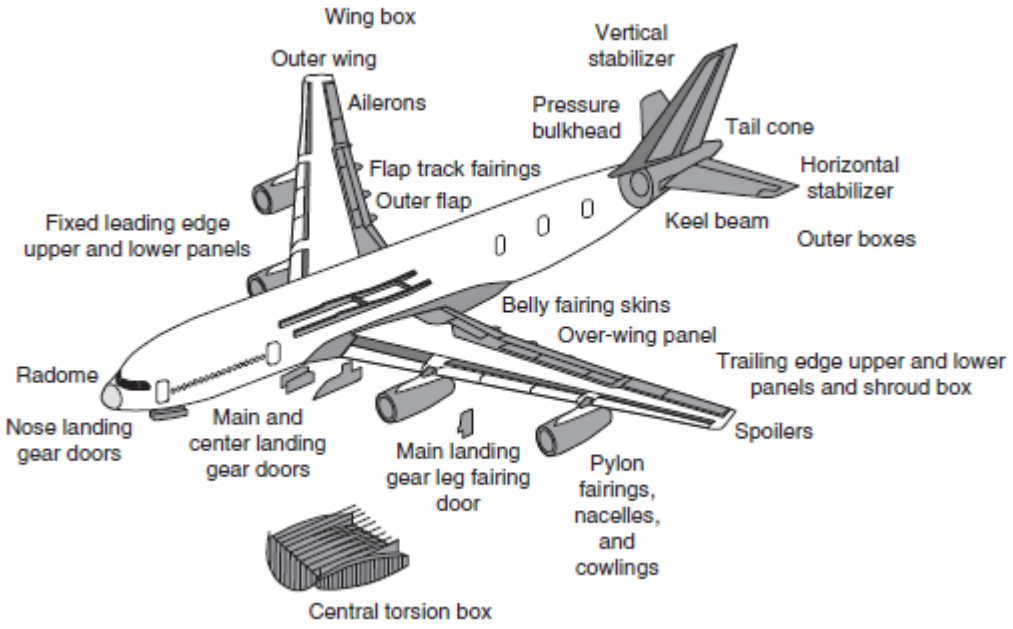

Figure 2.5. Use of fiber-reinforced polymer composites in Airbus 380
(Source: Mallick 2007)

CHAPTER 3

MECHANICS OF COMPOSITE MATERIALS

Many engineers and material scientists have adequate knowledge of the behavior and design of isotropic materials, which include the family of most metals and pure polymers. The rapidly increasing use of anisotropic materials such as composite materials has ended up with a materials revolution and it requires a new knowledge base of anisotropic material behavior.

The use of fiber-reinforced composite materials is different compared to conventional materials in application because the use of long fibers results in a material which has a higher strength-to-density ratio and/or stiffness-to-density ratio than any other material system at moderate temperature, and there exists the opportunity to uniquely tailor the fiber orientations to a given geometry, applied load and environment. For short fiber composites, used mainly in mass-production and low cost systems, the use of fibers makes the composites competitive and superior to plastic and metal alternative materials. For this reason through the use of composite materials, an engineer is not only a material selector, but is also a material designer (Vinson 2004). On the other hand, fiber-reinforced composites are microscopically inhomogeneous and orthotropic. Consequently, the mechanics of fiber-reinforced composites are more complicated than that of conventional materials (Mallick 2007).

3.1. Classical Lamination Theory

Classical lamination theory is based on classical plate theory and only valid for thin laminates. It is used to analyze the infinitesimal deformation of laminated structures. In this theory, it is assumed that laminate is thin and wide, perfect bounding exists between laminas, there exist a linear strain distribution through the thickness, all laminas are macroscopically homogeneous and behave in a linearly elastic manner, and the through the thickness strains and the transverse shear strains are zero (Kaw 2006). Thin laminated composite structure subjected to mechanical in-plane loading (N_x, N_y) considered in this thesis is shown in Figure 3.1. Cartesian coordinate system x, y and z

defines global coordinates of the layered material. A layer-wise principal material coordinate system is denoted by 1, 2, 3 and fiber direction is oriented at angle θ to the x axis. Representation of laminate convention for the n-layered structure with total thickness h is given in Figure 3.2.

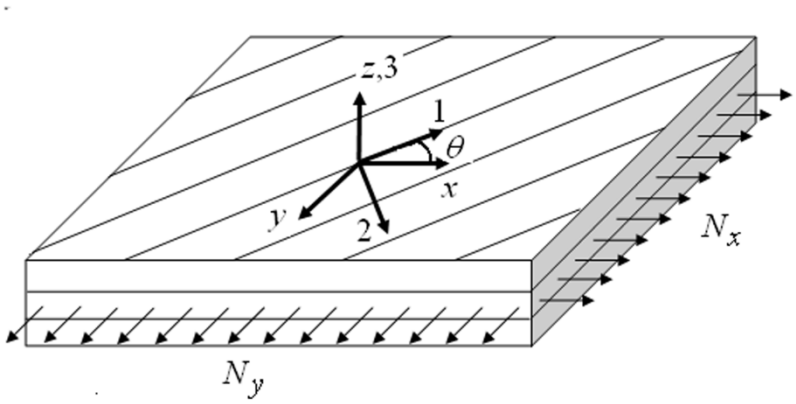

Figure 3.1. A thin fiber-reinforced laminated composite subjected to in plane loading

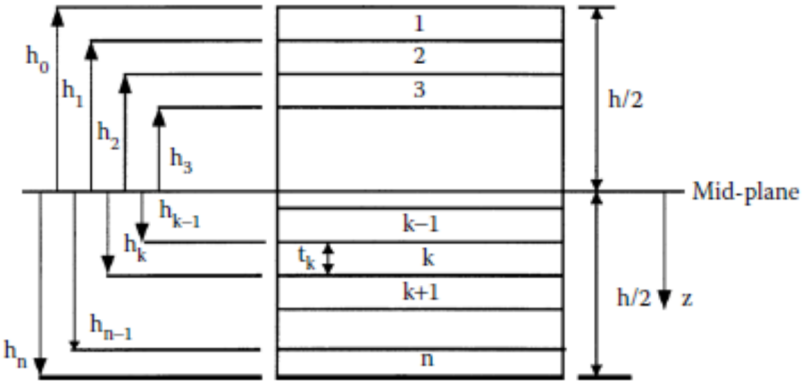

Figure 3.2. Coordinate locations of plies in a laminate
(Source: Kaw 2006)

In most structural applications, composite materials are used in the form of thin laminates loaded in the plane of the laminate. Consequently, composite laminates can be considered to be under a condition of plane stress with all stress components in the out-of-plane direction (3-direction) being zero.

The stress-strain relation for the k-th layer of a composite plate based on the classical lamination theory can be written in the following form

$$\begin{bmatrix} \sigma_x \\ \sigma_y \\ \sigma_{xy} \end{bmatrix}_k = \begin{bmatrix} \overline{Q}_{11} & \overline{Q}_{12} & \overline{Q}_{16} \\ \overline{Q}_{12} & \overline{Q}_{22} & \overline{Q}_{26} \\ \overline{Q}_{16} & \overline{Q}_{26} & \overline{Q}_{66} \end{bmatrix}_k \left(\begin{bmatrix} \varepsilon_x^o \\ \varepsilon_y^o \\ \varepsilon_{xy}^o \end{bmatrix} + z \begin{bmatrix} \kappa_x \\ \kappa_y \\ \kappa_{xy} \end{bmatrix} \right)_k \tag{3.1}$$

where $[\overline{Q}_{ij}]_k$ are the elements of the transformed reduced stiffness matrix, $[\varepsilon^o]$ is the mid-plane strains, $[\kappa]$ is curvatures, respectively.

The elements of transformed reduced stiffness matrix $[\overline{Q}_{ij}]$ given in Equation 3.1 can be expressed as in the following form

$$\overline{Q}_{11} = Q_{11}c^4 + Q_{22}s^4 + 2(Q_{12} + 2Q_{66})s^2c^2 \tag{3.2}$$

$$\overline{Q}_{12} = (Q_{11} + Q_{22} - 4Q_{66})s^2c^2 + Q_{12}(c^4 + s^4) \tag{3.3}$$

$$\overline{Q}_{22} = Q_{11}s^4 + Q_{22}c^4 + 2(Q_{12} + 2Q_{66})s^2c^2 \tag{3.4}$$

$$\overline{Q}_{16} = (Q_{11} - Q_{12} - 2Q_{66})sc^3 - (Q_{22} - Q_{12} - 2Q_{66})s^3c \tag{3.5}$$

$$\overline{Q}_{26} = (Q_{11} - Q_{12} - 2Q_{66})cs^3 - (Q_{22} - Q_{12} - 2Q_{66})sc^3 \tag{3.6}$$

$$\overline{Q}_{66} = (Q_{11} + Q_{22} - 2Q_{12} - 2Q_{66})s^2c^2 + Q_{66}(c^4 + s^4) \tag{3.7}$$

where stiffness matrix quantities $[Q_{ij}]$ are

$$Q_{11} = \frac{E_1}{1 - \nu_{21}\nu_{12}} \tag{3.8}$$

$$Q_{12} = \frac{\nu_{12} E_2}{1 - \nu_{21}\nu_{12}} \tag{3.9}$$

$$Q_{22} = \frac{E_2}{1 - \nu_{21}\nu_{12}} \tag{3.10}$$

$$Q_{66} = G_{12} \tag{3.11}$$

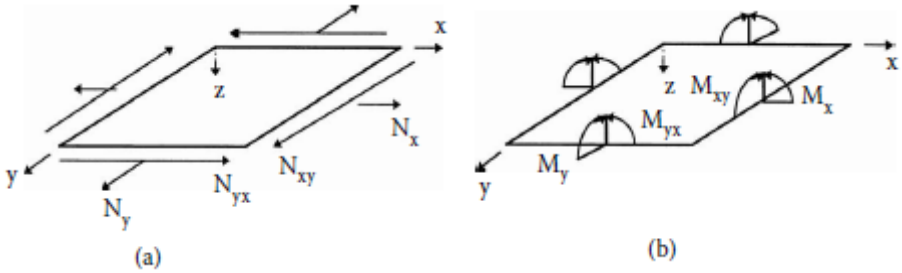

Figure 3. 3. Resultant forces and moments on a laminate
(Source: Kaw 2006)

Applied normal force resultants N_x, N_y, shear force resultant N_{xy} (per unit width) and moment resultants M_x, M_y and M_{xy} on a laminate (Fig. 3.3) have the following relations:

$$\begin{bmatrix} N_x \\ N_y \\ N_{xy} \end{bmatrix} = \begin{bmatrix} A_{11} & A_{12} & A_{16} \\ A_{12} & A_{22} & A_{26} \\ A_{16} & A_{26} & A_{66} \end{bmatrix} \begin{bmatrix} \varepsilon_x^0 \\ \varepsilon_y^0 \\ \gamma_{xy}^0 \end{bmatrix} + \begin{bmatrix} B_{11} & B_{12} & B_{16} \\ B_{12} & B_{22} & B_{26} \\ B_{16} & B_{26} & B_{66} \end{bmatrix} \begin{bmatrix} \kappa_x \\ \kappa_y \\ \kappa_{xy} \end{bmatrix} \tag{3.12}$$

$$\begin{bmatrix} M_x \\ M_y \\ M_{xy} \end{bmatrix} = \begin{bmatrix} B_{11} & B_{12} & B_{16} \\ B_{12} & B_{22} & B_{26} \\ B_{16} & B_{26} & B_{66} \end{bmatrix} \begin{bmatrix} \varepsilon_x^0 \\ \varepsilon_y^0 \\ \gamma_{xy}^0 \end{bmatrix} + \begin{bmatrix} D_{11} & D_{12} & D_{16} \\ D_{12} & D_{22} & D_{26} \\ D_{16} & D_{26} & D_{66} \end{bmatrix} \begin{bmatrix} \kappa_x \\ \kappa_y \\ \kappa_{xy} \end{bmatrix} \tag{3.13}$$

The matrices [A], [B] and [D] specified in Equations 3.14, 3.15, 3.16 can be defined as

$$A_{ij} = \sum_{k=1}^{n} [(\overline{Q}_{ij})]_k (h_k - h_{k-1}), \quad i, j = 1,2,6 \tag{3.14}$$

$$B_{ij} = \frac{1}{2} \sum_{k=1}^{n} [(\overline{Q}_{ij})]_k (h_k^2 - h_{k-1}^2), \quad i, j = 1,2,6 \tag{3.15}$$

$$D_{ij} = \frac{1}{3} \sum_{k=1}^{n} [(\overline{Q}_{ij})]_k (h_k^3 - h_{k-1}^3), \quad i, j = 1,2,6 \tag{3.16}$$

The [A], [B], and [D] matrices are called the extensional, coupling, and bending stiffness matrices, respectively. Combining Equation 3.12 and Equation 3.13 gives six simultaneous linear equations and six unknowns as:

$$\begin{bmatrix} N_x \\ N_y \\ N_{xy} \\ M_x \\ M_y \\ M_{xy} \end{bmatrix} = \begin{bmatrix} A_{11} & A_{12} & A_{16} & B_{11} & B_{12} & B_{16} \\ A_{12} & A_{22} & A_{26} & B_{12} & B_{22} & B_{26} \\ A_{16} & A_{26} & A_{66} & B_{16} & B_{26} & B_{66} \\ B_{11} & B_{12} & B_{16} & D_{11} & D_{12} & D_{16} \\ B_{12} & B_{22} & B_{26} & D_{12} & D_{22} & D_{26} \\ B_{16} & B_{26} & B_{66} & D_{16} & D_{26} & D_{66} \end{bmatrix} \begin{bmatrix} \varepsilon_x^0 \\ \varepsilon_y^0 \\ \gamma_{xy}^0 \\ \kappa_x \\ \kappa_y \\ \kappa_{xy} \end{bmatrix} \tag{3.17}$$

The extensional stiffness matrix [A] relates the resultant in-plane forces to the in-plane strains, and the bending stiffness matrix [D] relates the resultant bending moments to the plate curvatures. The coupling stiffness matrix [B] couples the force and moment terms to the mid-plane strains and mid-plane curvatures (Kaw 2006).

Now, stresses and strain expressions based on classical lamination theory can be expressed by local coordinate system (1, 2). The relation between the local and global stresses in an angled lamina can be written as in the following form:

$$\begin{bmatrix} \sigma_1 \\ \sigma_2 \\ \sigma_{12} \end{bmatrix} = [T] \begin{bmatrix} \sigma_x \\ \sigma_y \\ \sigma_{xy} \end{bmatrix} \tag{3.18}$$

Similarly, the local and global strains are also related as follows

$$\begin{bmatrix} \varepsilon_1 \\ \varepsilon_2 \\ \varepsilon_{12} \end{bmatrix} = [R][T][R]^{-1} \begin{bmatrix} \varepsilon_x \\ \varepsilon_y \\ \varepsilon_{xy} \end{bmatrix} \tag{3.19}$$

where

$$[R] = \begin{bmatrix} 1 & 0 & 0 \\ 0 & 1 & 0 \\ 0 & 0 & 2 \end{bmatrix} \tag{3.20}$$

and $[T]$ transform matrix,

$$[T] = \begin{bmatrix} c^2 & s^2 & 2sc \\ s^2 & c^2 & -2sc \\ -sc & sc & c^2 - s^2 \end{bmatrix} \qquad c = \cos\theta, \quad s = \sin\theta \tag{3.21}$$

3.2. Buckling Theory of Laminated Composite Plates

Assuming that the composite plate under consideration (Figure 3.1) is loaded by λN_x, λN_y and λN_{xy} in-plane compressive loads, where λ is a scalar amplitude parameter and simply supported on four sides, the governing differential equation for the buckling behavior of the plate, considering the classical plate theory, is

$$D_{11}\frac{\partial^4 w}{\partial x^4} + 2(D_{12} + 2D_{66})\frac{\partial^4 w}{\partial x^2 \partial y^2} + D_{22}\frac{\partial^4 w}{\partial y^4} = \lambda\left(N_x \frac{\partial^2 w}{\partial x^2} + N_y \frac{\partial^2 w}{\partial y^2} + N_{xy}\frac{\partial^2 w}{\partial x \partial y}\right) \tag{3.22}$$

where D_{11}, D_{12}, D_{22}, D_{66} are the terms of bending stiffnesses, w is the vertical displacement given by

$$w(x,y) = \sum_m \sum_n A_{mn} \sin\frac{m\pi x}{a} \sin\frac{n\pi y}{b} \tag{3.23}$$

With the substitution of Equation 3.23 to Equation 3.22, buckling load factor expression can be obtained as in the following form

$$\lambda_b = \frac{\pi^2\left[D_{11}\left(\frac{m}{a}\right)^4 + 2\left(D_{12}+2D_{66}\right)\left(\frac{m}{a}\right)^2\left(\frac{n}{b}\right)^2 + D_{22}\left(\frac{n}{b}\right)^4\right]}{N_x\left(\frac{m}{a}\right)^2 + N_y\left(\frac{n}{b}\right)^2 + N_{xy}\left(\frac{m}{a}\right)\left(\frac{n}{b}\right)} \tag{3.24}$$

A remarkable point is that D_{16} and D_{26} do not appear in Equation 3.22 and 3.23, because they are zero for a specially orthotropic laminate and they are small compared to the other D_{ij}'s for a symmetric laminate with a number of laminas of $\pm\theta$ ply angles in sequence (Karakaya and Soykasap 2009).

The laminate buckles into m and n half-waves in the x and y directions, respectively, when the magnitude parameter reaches a critical value of λ_b (Spallino and Thierauf 2000). The critical buckling load factor λ_{cb} limits the maximum load which the laminate can withstand without buckling and it is the smallest value of λ_b under appropriate m and n values. Unless the plate has a very high aspect ratio or extreme ratios of D_{ij}'s, the critical values of m and n are small (Gurdal, et al 1999). The critical buckling load factor λ_{cb} varies with the plate aspect ratio, loading ratio and material, and should be greater than one to avoid any immediate failure

$$\lambda_{cb} = \min \lambda_b(m,n) \tag{3.25}$$

The optimization problem which we have considered in the thesis study is to find the optimum configurations of composite plates which have the maximum critical buckling load factors, λ_{cb}. The values of m and n are taken to be 1 or 2 in order to result in a good estimate of buckling load capacity. Accordingly, the smallest of $\lambda_b(1,1)$, $\lambda_b(1,2)$, $\lambda_b(2,1)$, $\lambda_b(2,2)$ yields λ_{cb} in our thesis (Erdal and Sonmez 2005).

After obtaining the critical buckling load factor once, critical buckling loads can be determined by means of $N_{x,cr} = \lambda_{cb} N_x$ and $N_{y,cr} = \lambda_{cb} N_y$ expressions.

CHAPTER 4

FAILURE THEORIES IN COMPOSITE PLATES

Weight minimization of composite plates necessarily includes strength constraints because decreasing number of load carrying plies ultimately causes failure. Composite structures must be able to resist the imposed loads without affecting any failure. Consequently, the research field of failure criteria for fiber-reinforced plastic composites has attracted attention of many researchers over the last few decades. Various types of approaches which clearly prove that failure criteria for fiber-reinforced composites have been presented in the literature and this subject is still an important research issue in composite structures.

With respect to failure criteria of composite plates, they can be categorized into three classes: limit or non-interactive theories (e.g., Maximum stress or maximum strain), interactive theories (e.g., Tsai-Hill, Tsai-Wu or Hoffman) and partially interactive or failure mode-based theories (e.g., Hashin, Puck failure criterion (PFC)) (Lopez, et al. 2009).

4.1.Traditional Failure Theories

Firstly, it is necessary to be mentioned about commonly used failure criteria for polymer-matrix composites. These are the maximum stress and the Tsai-Wu criterion. These failure theories assume that failure occurs only in the fiber direction.

4.1.1. Maximum Stress Theory

Failure analysis of laminated composites is generally based on the stresses in each lamina in the principal material coordinates. With regard to the maximum normal stress theory by Rankine and the maximum shearing stress theory by Tresca, this theory is similar to those applied to isotropic materials. The stresses acting on a lamina are resolved into the normal and shear stresses in the local axes. According to the maximum

stress theory, failure occurs when a maximum stress in the principal material coordinates exceeds the respective strength. This is expressed as,

$$\sigma_1 \geq X_T \quad \text{or} \quad \sigma_2 \geq Y_T \quad \text{(for tensile stresses)} \tag{4.1}$$

$$\sigma_1 \leq -X_C \quad \text{or} \quad \sigma_2 \leq -Y_C \quad \text{(for compressive stresses)} \tag{4.2}$$

$$\left|\tau_{12}\right| \geq S_{12} \quad \text{or} \quad \text{(for shearing stresses)} \tag{4.3}$$

where σ_1 and σ_2 are the normal stresses in the directions 1 and 2, respectively; S_{12} is the shear stress in the elastic symmetry plane 1-2; X_T and X_C are the tensile and compressive strengths parallel to the fiber direction, respectively; Y_T and Y_C are the tensile and compressive strengths normal to the fiber direction, respectively; and S_{12} is the shear strength. Note that, X_T, X_C, Y_T, Y_C and S_{12} are positive quantities.

4.1.2. Tsai-Wu Failure Criterion

The Tsai–Wu criterion is proposed for use with orthotropic materials. It is derived from the von Mises yield criterion and based on the total strain energy failure theory of Beltrami. Tsai-Wu applied the failure theory to a lamina in plane stress. A lamina is considered to be failed if

$$F_{11}\sigma_1^2 + F_1\sigma_1 + F_2\sigma_2 + 2F_{12}\sigma_1\sigma_2 + F_{22}\sigma_2^2 + F_{21}\tau_{12}^2 < 1 \tag{4.4}$$

is violated. F_{ij} are called the strength coefficients and are given by

$$F_1 = \frac{1}{X_T} - \frac{1}{X_C} \; ; \; F_2 = \frac{1}{Y_T} - \frac{1}{Y_C} \; ;$$

$$F_{11} = \frac{1}{X_T X_C} \; ; \; F_{22} = \frac{1}{Y_T Y_C} \; ; \; F_{12} \cong -\frac{1}{2}\sqrt{F_{11}F_{22}}$$

4.2. Puck Failure Criterion (PFC)

The Puck Failure Theory of composite plates relies on Mohr's hypothesis which fracture is caused exclusively by the stresses acting on the fracture plane. PFC includes two main failure modes:

- Fiber Failure (FF)
- The Inter-Fiber failure (IFF)

4.2.1. Puck Fiber Failure (FF)

Fiber failure is based on the assumption that failure under multiaxial stresses (σ_{f1}, σ_{f2}) occurs at the same threshold level at which failure occurs for uniaxial stresses. After some improvement, Puck and Schürmann found that failure occurs if one of the following conditions is satisfied:

For tensile stresses,

$$\frac{1}{\varepsilon_{1T}}\left(\varepsilon_1 + \frac{\nu_{f12}}{E_{f1}} m_{\sigma f} \sigma_2\right) = 1 \qquad \text{for} \quad S \geq 0 \tag{4.5}$$

For compressive stresses,

$$\frac{1}{\varepsilon_{1C}}\left|\left(\varepsilon_1 + \frac{\nu_{f12}}{\varepsilon_{f1}} m_{\sigma f} \sigma_2\right)\right| + \left(10\gamma_{21}\right)^2 = 1 \qquad \text{for} \quad S < 0 \tag{4.6}$$

in which,

$$S = \left(\varepsilon_1 + \frac{\nu_{f12}}{E_{f1}} m_{\sigma f} \sigma_2\right)$$

where ε_{1T} and ε_{1C} are tensile and compressive failure strains in direction 1, respectively; ε_1 is the normal strain in the direction 1; ν_{f12} is the Poisson's ratio of the

fibers (the ratio of the strain in direction 2 to the strain in direction 1, both of which are caused by a stress in direction 1 only); $m_{\sigma f}$ accounts for a stress-magnification effect caused by the different moduli of the fibers and matrix (in direction 2), which leads to an uneven distribution of the stress σ_2 from a micromechanical point of view; E_{f1} is the Young's modulus of the fiber in direction 1; and γ_{21} is the shear strain in the plane 1-2, in which $(10\gamma_{21})^2$ is an empirical shear correction. Note that $S \geq 0$ corresponds to tension, while $S < 0$ corresponds to compression.

4.2.2. Puck Inter-Fiber Failure (IFF)

Contrary to dealing with the principal material coordinates (Figure 4.1), Inter-fiber failure equations are derived based on the axes corresponding to the failure plane. These axes are shown in Figure 4.2, where θ_{fp} represents the angle at which failure occurs.

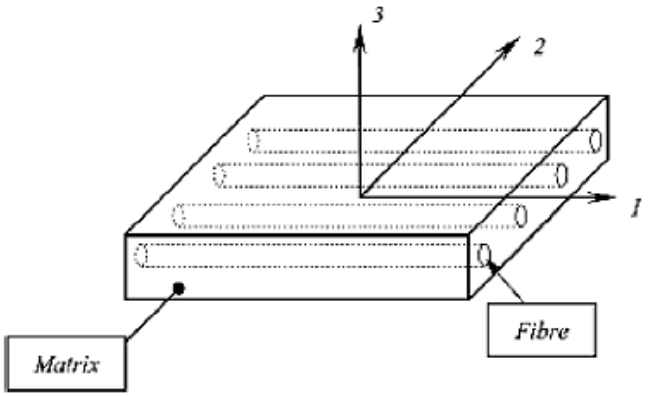

Figure 4.1. Principal material coordinates of a typical lamina
(Source: Lopez, et al. 2009)

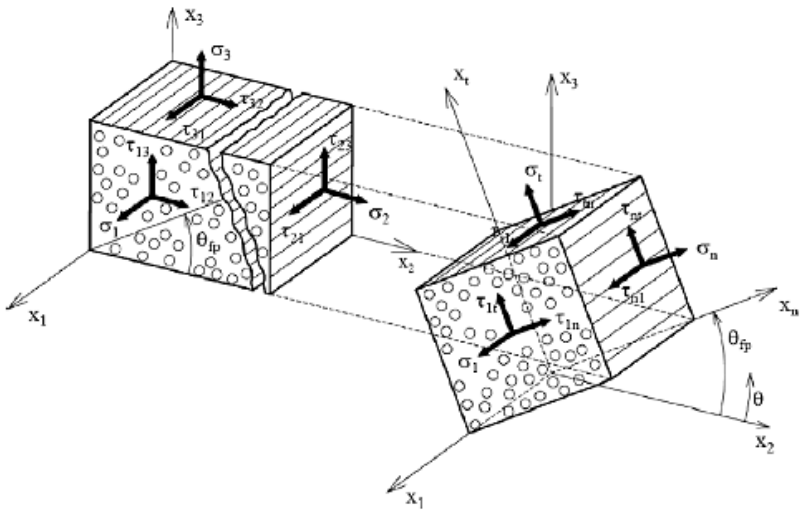

Figure 4.2. Three-dimensional stresses on a UD composite element. (x_1, x_2, x_3) coordinate system is fixed to fiber direction (x_1), laminate mid-surface (x_2) and thickness direction (x_3). The (x_1, x_n, x_t) coordinate system is rotated by an angle θ_{fp} from the x_2 direction to the x_n direction which is normal to the fracture plane. The inter-fiber fracture is influenced by the the three stresses σ_n, τ_{nt}, τ_{n1} only (according to Mohr's strength theory) (Source: Puck and Schürmann 1998)

The PFC provides not only a failure factor, but also the inclination of the plane where failure will possibly occur; consequently it allows a much better assessment of the consequences of Inter Fiber Failure in the laminate. IFF is subdivided into three failure modes, which are referred to as A, B and C. These are shown in Figure 4.3.

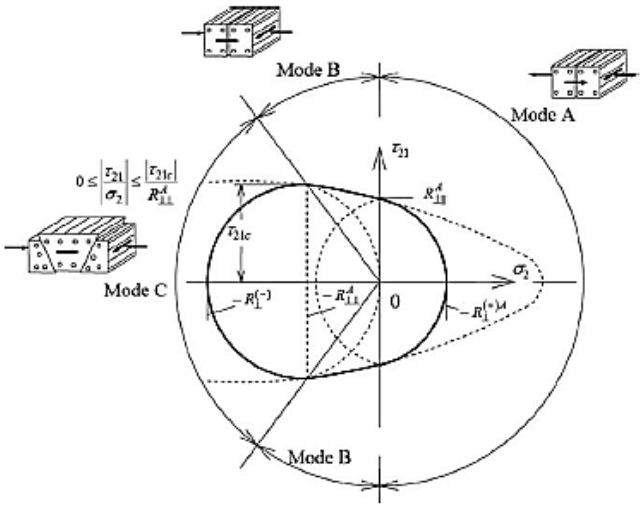

Figure 4.3. (σ_2, τ_{21}) fracture curve for σ_1, representing the three different fracture modes (A, B and C) for the PFC (Source: Lopez, et al. 2009)

Mode A occurs when the lamina is subjected to tensile transverse stress; however mode B and mode C correspond to compressive transverse stress. The classification of modes is based upon the idea that a tensile stress $\sigma_n > 0$ leads to fracture, while a compressive stress $\sigma_n < 0$ prevents shear fracture. For $\sigma_n < 0$, the shear stresses τ_{nt} and τ_{n1} (or just one of them) have to face an additional fracture resistance, which increases $|\sigma_n|$, with analogously to an internal friction. The difference between mode B and C is based on their failure angles and these angles are 0° for mode B and a different value for mode C. Additionally, failure mode C is considered more serious because it produces inclined cracks and may lead to delamination of layers.
The Puck Inter-Fiber Failure mode A, B and C are determined as follows:

Mode A ($\theta_{fp}=0°$)

Failure condition effort (effort $f_{E(FF)}$ *or* $f_{E(IFF)}$) Condition for validity

$$\sqrt{\left(\frac{\tau_{21}}{S_{21}}\right)^2+\left(1-p_{\perp\parallel}^{(+)}\frac{\gamma_T}{S_{21}}\right)^2\left(\frac{\sigma_2}{Y_T}\right)^2}+p_{\perp\parallel}^{(+)}\frac{\sigma_2}{S_{21}}=1-\left|\frac{\sigma_1}{\sigma_{1D}}\right| \qquad \sigma_2\geq 0 \qquad (4.7)$$

Mode B ($\theta_{fp}=0°$)

Failure condition effort (effort $f_{E(FF)}$ *or* $f_{E(IFF)}$) Condition for validity

$$\frac{1}{S_{21}}\left(\sqrt{\tau_{21}{}^2+\left(p_{\perp\parallel}^{(-)}\sigma_2\right)^2}+p_{\perp\parallel}^{(-)}\sigma_2\right)=1-\left|\frac{\sigma_1}{\sigma_{1D}}\right| \qquad \sigma_2<0 \text{ and } 0\leq\left|\frac{\sigma_2}{\tau_{21}}\right|\leq\frac{R_{\perp\perp}^A}{|\tau_{21c}|} \qquad (4.8)$$

Mode C $\left(\theta_{fp}=\arccos\sqrt{\frac{f_w R_{\perp\perp}^A}{(-\sigma_2)}}\right)$

Failure condition effort (effort $f_{E(IFF)}$) Condition for validity

$$\left[\left(\frac{\tau_{21}}{2\left(1+p_{\perp\perp}^{(-)}\right)S_{21}}\right)^2+\left(\frac{\sigma_2}{Y_C}\right)^2\right]\frac{Y_C}{(-\sigma_2)}=1-\left|\frac{\sigma_1}{\sigma_{1D}}\right| \qquad \sigma_2<0 \text{ and } 0\leq\left|\frac{\tau_{21}}{\sigma_2}\right|\leq\frac{|\tau_{21c}|}{R_{\perp\perp}^A} \qquad (4.9)$$

where the weakening factor $f_w=\left(0.9f_{E(FF)}\right)^n$ is for the degradation effect of σ_1 and n depends on the matrix of the laminate (for example, $n=6$ for epoxy).

As seen in the equations, there are some new parameters which come from the theory. Their definitions and parameter relationships are given as

Definitions

$$p_{\perp\parallel}^{(+)}=-\left(\frac{d\tau_{21}}{d\sigma_2}\right)_{\sigma_2=0} \quad of\ (\sigma_2,\tau_{21})\ curve, \quad \sigma_2\geq 0$$

$$p_{\perp\parallel}^{(-)}=-\left(\frac{d\tau_{21}}{d\sigma_2}\right)_{\sigma_2=0} \quad of\ (\sigma_2,\tau_{21})\ curve, \quad \sigma_2\leq 0$$

Parameter relationships

$$R_{\perp\perp}^{A}=\frac{Y_C}{2\left(1+p_{\perp\perp}^{(-)}\right)}=\frac{S_{21}}{2p_{\perp\parallel}^{(-)}}\left(\sqrt{1+2p_{\perp\parallel}^{(-)}\frac{Y_C}{S_{21}}}-1\right)$$

$$p_{\perp\perp}^{(-)}=p_{\perp\parallel}^{(-)}\frac{R_{\perp\perp}^{A}}{S_{21}}$$

$$\tau_{21c}=S_{21}\left(\sqrt{1+2p_{\perp\perp}^{(-)}}\right)$$

The use of criteria that closely reflect the actual behavior of the laminated composites under study is critical. Many studies related to optimal composite design use generally failure criteria based on the von Mises or Hill yield criteria, which are more suitable for ductile materials. Essentially, as the failure behavior of composite parts is similar to brittle materials, it is more appropriate to use criteria conformed to materials that include brittle fractures, such as Mohr's criterion. Therefore, Puck failure criterion was taken into account in the thesis.

CHAPTER 5

OPTIMIZATION

5.1. Introduction

Optimization is commonly used, from engineering design to financial markets, from our daily activity to planning our holidays, and computer sciences to industrial applications. People always tend to maximize or minimize something. In fact, we are continuously searching for the optimal solutions to every problem we face, however we are not necessarily able to find such solutions (Xin-SheYang 2010).

The modern optimization methods have come up as powerful and popular methods for solving complex engineering optimization problems in recent years. Example of these optimization methods are genetic algorithm, simulated annealing, particle swarm optimization, ant colony optimization, neural network-based optimization, and fuzzy optimization.

One of the most used optimization methods, the genetic algorithm is computerized search and optimization algorithm based on the mechanics of natural genetics and natural selection. The genetic algorithms were initially proposed by John Holland in 1975.

Optimization is the act of obtaining the best result under given conditions. The ultimate purpose in design of any engineering system is either to minimize the effort required or to maximize the desired benefit. Since the effort required or the benefit anticipated in any practical situation can be expressed as a function of certain decision variables, optimization can be defined as the process of finding the conditions that give the maximum or minimum value of a function. It can be seen from Figure 5.1 that if a point x^* corresponds to the minimum value of function $f(x)$, the same point also corresponds to the maximum value of the negative of the function, $-f(x)$. Consequently, without loss of generality, optimization can be taken to mean minimization because the maximum of a function can be found by searching for the minimum of the negative of the same function (Rao 2009).

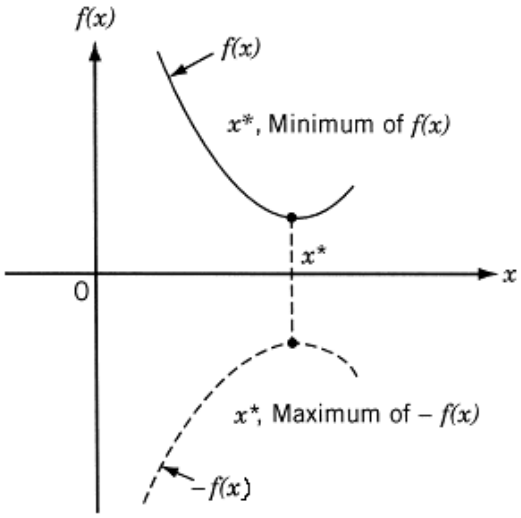

Figure 5.1. Minimum and maximum of objective function (*f(x)*)
(Source: Rao 2009)

Table 5.1 generally classifies optimization techniques by listing various mathematical programming techniques together with other well-defined areas of operations research.

Table 5.1. Methods of Operations Research
(Source: Rao 2009)

Mathematical programming or optimization techniques	Stochastic process techniques	Statistical methods
Calculus methods	Statistical decision theory	Regression analysis
Calculus of variations	Markov processes	Cluster analysis, pattern recognition
Nonlinear programming	Queueing theory	
Geometric programming	Renewal theory	Design of experiments
Quadratic programming	Simulation methods	Discriminate analysis (factor analysis)
Linear programming	Reliability theory	
Dynamic programming		
Integer programming		
Stochastic programming		
Separable programming		
Multiobjective programming		
Network methods: CPM and PERT		
Game theory		
Modern or nontraditional optimization techniques		
Genetic algorithms		
Simulated annealing		
Ant colony optimization		
Particle swarm optimization		
Neural networks		
Fuzzy optimization		

The optimization techniques are practical in finding the minimum of a function of several variables under a described set of constraints. Stochastic search techniques can be used to analyze problems defined by a set of random variables having known probability distributions. Statistical methods allow one to analyze the experimental data and build empirical models to achieve the most accurate representation of the physical situation. Genetic Algorithms which we are interested in are in the modern optimization techniques category and the most commonly used one (Rao 2009).

5.2. Definition of Optimization Problem

An optimization or a mathematical programming problem can be defined as follows

$$\text{Find } X = \begin{Bmatrix} x_1 \\ x_2 \\ \vdots \\ x_n \end{Bmatrix} \text{ which minimizes } f(x) \tag{5.1}$$

subject to the constraints

$$g_i(X) \le 0, \qquad i = 1, 2, \ldots, m$$
$$l_i(X) = 0, \qquad i = 1, 2, \ldots, p$$

where X is an n-dimensional vector called the design vector, $f(X)$ is termed the objective function, and $g_i(X)$ and $l_i(X)$ are known as inequality and equality constraints, respectively. The number of variables n and the number of constraints m and/or p are not necessary to be related in any way. The optimization problem stated in Equation 5.1 is called a constrained optimization problem. There are not any constraints in some optimization problems which are called unconstrained optimization problems (Rao 2009).

5.3. Genetic Algorithm (GA)

Evolutionary calculating was introduced in the 1960s by I. Rechenberg in the study “Evolution strategies”. Afterwards, this idea was developed by other researches. Genetic Algorithm (GA) was discovered by John Holland in 1975 and developed as a useful method for search and optimization problems (S.N.Sivanandam and S.N.Deepa 2008). GA is a class of evolutionary algorithms inspired by evolutionary biology.

GA is based on a natural selection process which ends up with the evolution of organisms best adapted to the environment. Genetic algorithm begins its search with a population of random individuals. Each member of the population holds a chromosome which encodes certain characteristics of the individual. The algorithm methodically analyzes each individual in the population of designs according to set specifications and assigns it a fitness rating which represents the designer’s aims. This fitness rating is then used to identify the structural designs which perform better than others. Thus, it enables the genetic algorithm to determine the designs which are weak and must be eliminated using the reproduction operator. After this step, the remaining, more desirable genetic material is utilized to create a new population of individuals. This part is carried out by applying two more operators similar to natural genetic processes, which called gene crossover and gene mutation. The process is iterated over many generations in order to obtain optimal designs. A flowchart practically summarizing the process of genetic algorithm is shown in Figure 5.2.

As the evolutionary algorithm technique, GA provides important benefits over traditional gradient based optimization routines, such as nominal insensitivity to problem complexity and the ability to discover easily global optimum rather than local optima (Pelletier and Vel 2006).

The ability of the algorithm to explore and exploit simultaneously, a growing amount of theoretical validation, and successful application to real-world problems strongly support the conclusion that genetic algorithm are a powerful, robust optimization technique (Sivanandam and Deepa 2008).

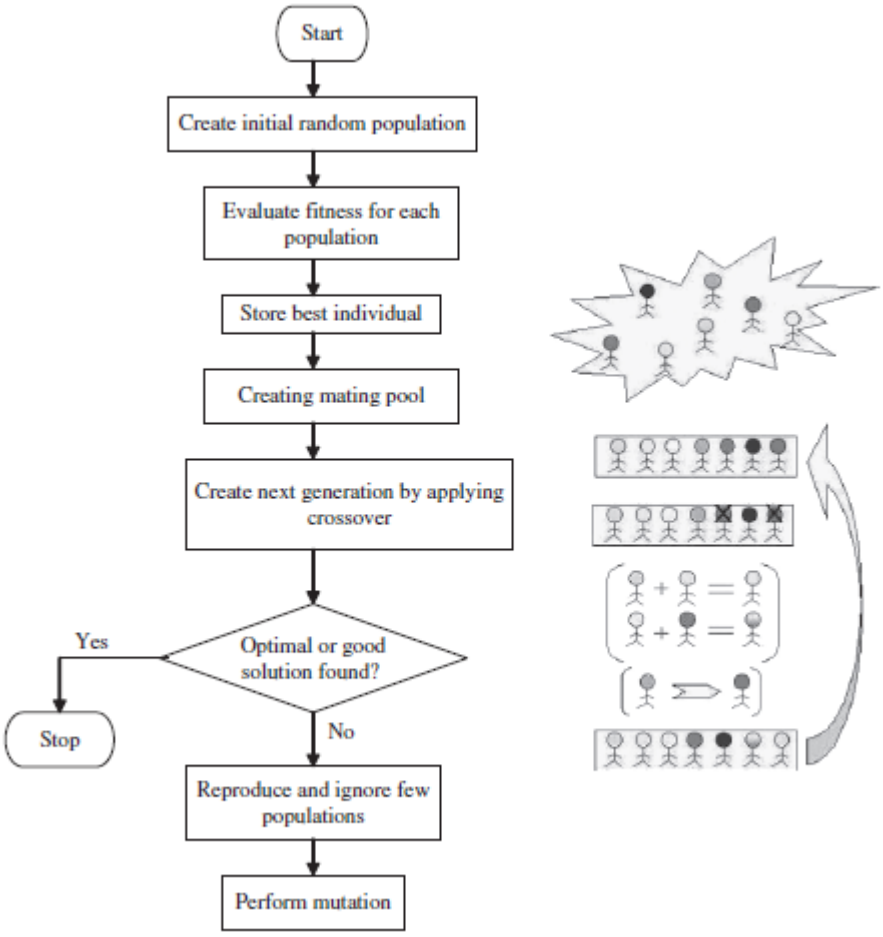

Figure 5.2. Flowchart of genetic algorithm
(Source: Sivanandam and Deepa 2008)

5.3.1. Terminology

The basic terminologies used in Genetic Algorithms to obtain a good enough solution for possible terminating conditions need to be defined at this point. The two distinct elements in the GA are individuals and populations. An individual is a single solution while the population is the set of individuals currently involved in the search process. Individual includes two forms of solutions. They are the chromosome, which is the raw 'genetic' information (genotype) that the GA deals and the phenotype, which expresses the chromosome in the terms of the model. A chromosome includes subsections of genes. A gene is the GA's representation of a single factor for a control factor. Each factor in the solution set corresponds to gene in the chromosome. Chromosomes are encoded by bit strings and an illustration is given below in Figure 5.3.

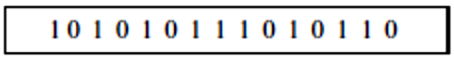

Figure 5.3. Representation of a chromosome

Genes are the basic "instructions" for building Generic Algorithms. A chromosome is a sequence of genes. A gene is a bit string of arbitrary lengths. In a chromosome, the genes are represented as in Figure 5.4.

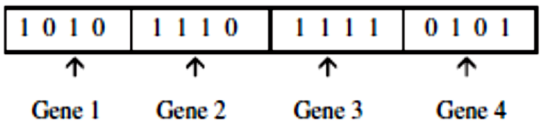

Figure 5.4. Representation of genes in a chromosome

The fitness of an individual in a genetic algorithm is the value of an objective function for its phenotype. For calculating fitness, the chromosome has to be first decoded and the objective function has to be evaluated. The fitness not only specifies how good the solution is, but also corresponds to how close the chromosome is to the optimal one.

A population consists of a group of individuals. The two important aspects of population used in Genetic Algorithms are initial population generation and population size. The search process consists of initializing the population and then breeding new individuals until the termination condition is satisfied (Sivanandam and Deepa 2008).

5.3.2. Breeding

The breeding process is the basis of the genetic algorithm. In this essential process, new and hopefully fitter individuals are created through the search procedure. The breeding cycle consists of three steps:

a) Selecting parents.
b) Crossing the parents to create new individuals (offspring or children).
c) Replacing old individuals in the population with the new ones.

5.3.2.1. Selection

Selection is the process of choosing two parents from the current population for crossing. After deciding on an encoding, the next step is to determine how to perform selection i.e., how to choose individuals in the population which will create offspring for the next generation and how many offspring each will create. The aim of selection is to highlight fitter individuals in the population in hopes that their off springs have higher fitness. Figure 5.5 shows the basic selection process. There are different selection methods such as roulette, random, rank, tournament or stochastic (Sivanandam and Deepa 2008).

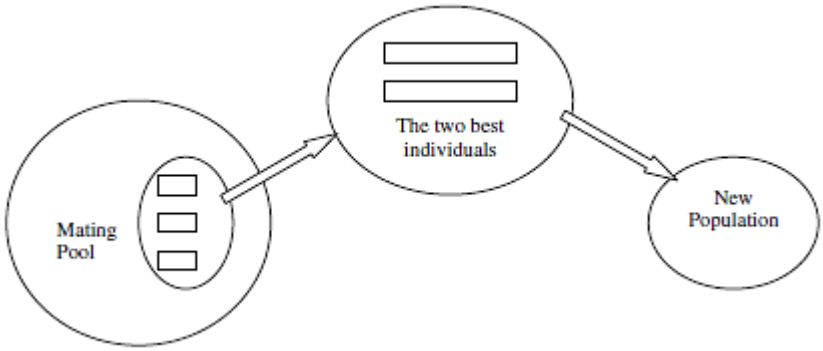

Figure 5.5. Selection process

5.3.2.2. Crossover (Recombination)

Crossover is one of the important GA operators which has basic task of creating new children in a reproduction process. This GA step performs combining genetic information taken from a pair of parents. Crossover is the process of taking two parent solutions and producing from them a child. After the selection (reproduction) process, the population is enriched with better individuals. Reproduction makes clones of good strings, however it does not create new ones. Crossover operator is applied to the mating pool with the hope that it creates a better offspring. First, the GA's crossover operator produces a random number to define the crossover point. Then, the gene strings of the related chromosomes are split at the same point in the parents. The left part of parent 1 and the right part of parent 2 are reorganized to create a child as seen in Figure 5.6 (Spall 2003; Sivanandam and Deepa 2008).

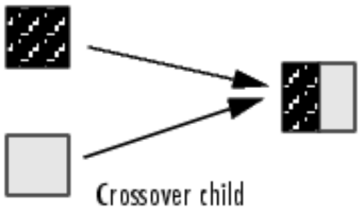

Figure 5.6. Crossover

5.3.2.3. Mutation

Mutation process is applied to the strings after crossover. Mutation is a genetic operator which maintains the genetic diversity from one generation of a population to the next generation. In mutation operation, the solution can change completely from the previous solution and so better solution can be obtained. The working principle of mutation is based on introducing of new genetic structures in the population by randomly modifying some of its building blocks. Mutation provides a random search capability to GA and this is useful to find areas which are close to the solution in the design space. Mutation prevents the algorithm to be trapped in a local minimum. There are many different forms of mutation for the different kinds of representation (Gurdal, et al. 1999; Sivanandam and Deepa 2008).

5.3.2.4. Replacement

Replacement is the last step of breeding cycle. In this GA step, two parents are drawn from a fixed size population, they breed two children, but not all four can return to the population, therefore two must be replaced. In other words, once offsprings are produced, a method must determine which of the current members of the population, if any, should be replaced by the new solutions. There are a few replacement situations. In random replacement, the children replace two randomly chosen individuals in the population. In weak parent replacement, a weaker parent is replaced by a strong child. In Both parents replacement, the child replaces the parent (Sivanandam and Deepa 2008).

5.4. MATLAB Optimization Toolbox

MATLAB *Genetic Algorithm and Direct Search, Symbolic Math Toolbox*es have been used in the thesis (The Mathworks, Inc. 2008). MATLAB *Genetic Algorithm and Direct Search Toolbox* includes commonly used algorithms which solves constrained and unconstrained continuous and discrete problems for standard and large-scale optimization. Some solvers in the toolbox are such as 'Constrained nonlinear minimization (fmincon)', 'Genetic Algorithm (ga)', 'Multiobjective optimization using Genetic Algorithm (gamultiobj)', 'Pattern Search (patternsearch)' or 'Simulated annealing algorithm (simulannealbnd)' and these solvers can be selected as an optimization algorithm from Optimization Tool GUI. These methods have also been used in design of composite materials by many researchers in the literature (Ozgur and Sonmez 2005; Karakaya and Soykasap 2009; Pelletier and Vel 2006). Genetic Algorithm solver has been used in this thesis.

5.4.1. Genetic Algorithm Solver (ga)

GA solver of the optimization toolbox consists of two main sections: Problem definition and Options. The Problem Setup and Results (problem definition) section includes Fitness function, Number of variables, Constraints and Bounds. The Options section includes some significant adjustments such as Population, Fitness scaling, Selection, Reproduction, Mutation, Crossover, Migration. A genetic algorithm solver interface is illustrated in Figure 5.7.

As seen in the figure, Fitness function and Number of variables should be defined firstly. Fitness function is the objective function to be minimized or maximized and Number of variables corresponds to the length of the input vector related to the fitness function. Constraints and/or a nonlinear constraint function can be entered for the problem in the Constraints panel. If the problem is unconstrained, these fields are left blank. The Start button is used to run the genetic algorithm. The results of the optimization are displayed in the Run solver and view results panel. The options of the genetic algorithm can be changed in the Options panel if needed.

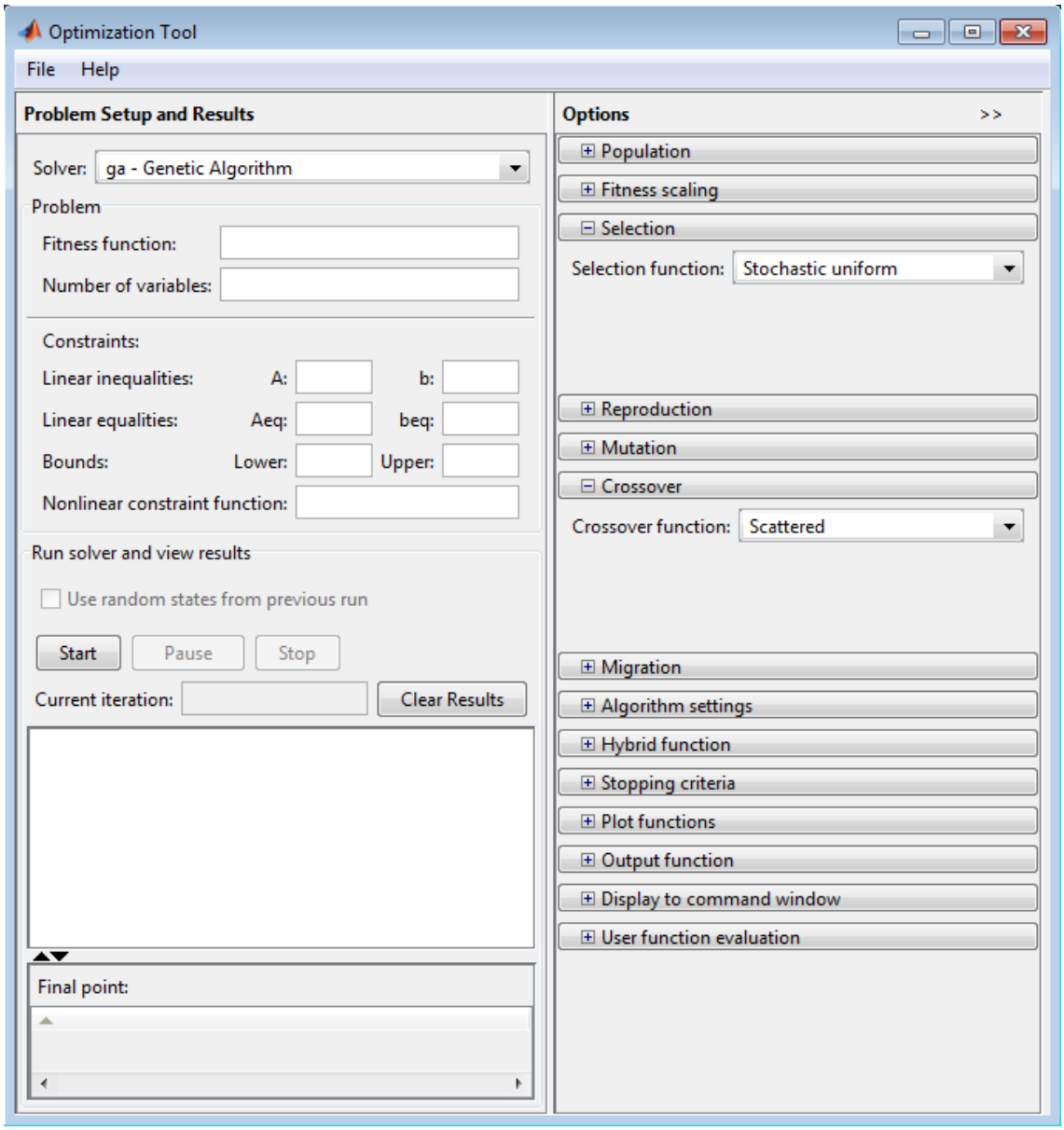

Figure 5.7. Matlab optimization toolbox ga solver user interface

To improve the reliability and obtain the best results from the genetic algorithm, it is necessary to be specified appropriate options for the genetic algorithm.

Population options enable you to specify the parameters of the population which the genetic algorithm uses and this section consists of Population type, Population size, Creation function, Initial population, Initial scores and Initial range. *Population type* specifies the type of the input to the fitness function. *Creation function* specifies the function which forms the initial population for genetic algorithm. *Population size* specifies the number of individuals in each generation. With a large population size, genetic algorithm searches the solution space more comprehensively, thereby reducing

the possibility which the algorithm will return a local minimum that is not global optima. However, a large population size also causes the algorithm to run more slowly. *Initial population* specifies an initial population for the genetic algorithm. *Initial scores* specifies initial scores for the initial population. *Initial range* specifies the range of the vectors in the initial population which is generated by a creation function.

In *Fitness scaling* section, the raw fitness scores which are returned by the fitness function are converted to values in a range which is suitable for the selection function. Scaling function specifies the function that performs the scaling. The options of *Fitness scaling* are *Rank*, *Proportional*, *Top*, *Shift linear* and *Custom*.

Selection option includes selection function such as *Uniform*, *Roulette*, *Tournament* and *Custom*. The purpose of using selection function is to determine parents for the next generation based on their scaled values from the objective functions. In order to achieve an ideal selection strategy, its selective pressure and population diversity should be adjusted.

Reproduction option is related to determination of Genetic Algorithm children creation at each new generation. In the toolbox, *Crossover fraction* is utilized as a sub-option and it specifies the fraction of the next generation that crossover produces. *Crossover fraction* must be a fraction between 0 and 1.

Mutation option has four different mutation functions such as *Constraint dependent*, *Gaussian*, *Uniform* and *Adaptive feasible*. If there are no constraints or bounds in the specified problem, *Gaussian* sub-option can be selected, otherwise *Adaptive feasible* should be used.

In *Crossover* option, the function which performs the crossover in the sub-option *Crossover function* should be specified. There exist following six different crossover functions in the toolbox: *Scattered*, *Single point*, *Two point*, *Intermediate*, *Heuristic* and *Arithmetic*.

Stopping criteria options enable you to specify the values of *Generations*, *Time limit*, *Fitness limit*, *Stall generations*, *Stall time limit*, *Function tolerance* and *Nonlinear constraint tolerance*. The algorithm stops as soon as any one of these conditions is met. Furthermore, *Plot functions* section enables you to display various plots which provide information about the genetic algorithm while it is running.

In Table 5.2, all genetic algorithm options in the toolbox used in the problems of this thesis are presented.

Table 5.2. Genetic Algorithm parameters used in optimization

Population Type	Double vector
Population size	40
Creation function	Use constraint dependent
Initial population	[ ]
Initial scores	[ ]
Initial range	[-90;90]
Scaling function	Rank
Selection function	Roulette
Elite count	2
Crossover fraction	0.6
Mutation function	Use constraint dependent
Crossover function	Scattered
Migration direction	Both Fraction = 0.2, Interval = 20
Initial penalty	10
Penalty factor	100
Hybrid Function	fmincon
Stopping criteria	Generations = 1000 Stall generations = 1000 Function tolerance = 10^{-6}

CHAPTER 6

RESULTS AND DISCUSSION

6.1. Problem Definition

Determination of the buckling load capacity of a composite plate under in-plane compressive loads is critical for the design of the composite structures because the buckling could yield a premature failure of the structure. Accordingly, the aim of the thesis is to obtain the best design of laminated composite plates in different loadings and plate dimensions, which could resist to buckling and satisfy the Puck failure criterion. The composite plates under consideration are rectangular, simply supported on four sides with length of a and width of b, and subjected to in-plane loads per unit length N_x and N_y, as shown in Figure 6.1.

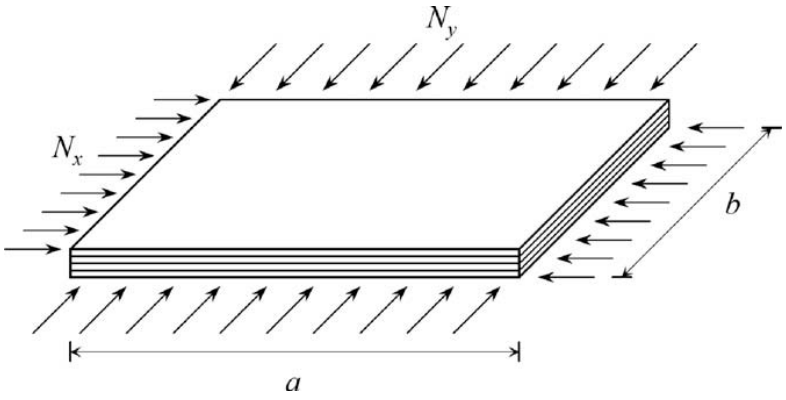

Figure 6.1. Laminated composite subjected to in-plane loads
(Source: Lopez, et al. 2009)

64-layered composite plates made of carbon/epoxy have been considered in the thesis. Each layer is 0.25 mm thick and the length of plate a equals to 0.508 m. N_x has been taken as 1000 N/mm, 3000 N/mm, 5000 N/mm and 10000 N/mm in the design process. N_y and b have been calculated from the load ratio (N_x / N_y) and the plate aspect ratio (a/b) accordingly. The elastic properties of the layers and the failure

properties of the lamina have been taken from a previous study (Lopez, et al. 2009) and given in Table 6.1 and Table 6.2.

Table 6.1. The elastic properties of carbon/epoxy layers
(Source: Lopez, et al. 2009)

Longitudinal Modulus	$E_1 = 116600$ MPa
Transverse Modulus	$E_2 = 7673$ MPa
In-plane shear modulus	$G_{12} = 4173$ MPa
Poisson's ratio	$\nu_{12} = 0.27$
Density	$\rho = 1605$ kg/m^3

Table 6.2. Strength properties of the lamina
(Source: Lopez, et al. 2009)

X_T	2062 MPa	Y_C	240 MPa	ε_{1T}	0.0175	$m_{\sigma f}$	1.1
X_C	1701 MPa	S_{21}	105 MPa	ε_{1C}	0.014	$p_{\perp /\!/}^{(-)}$	0.25
Y_T	70 MPa	E_{f1}	230000 MPa	ν_{f12}	0.23	$p_{\perp /\!/}^{(+)}$	0.3

The plate design has been studied under loading ratios; $N_x / N_y = 1$, $N_x / N_y = 2$, $N_x / N_y = 4$, $N_x / N_y = 1/2$ and plate aspect ratios; $a/b = 1$, $a/b = 2$, $a/b = 4$, $a/b = 1/2$. Fiber orientation angles of the plate have been taken as design variables and considered continuous ($-90 \le \theta \le 90$) during the optimization process. The composite plates considered in the thesis are symmetric and balanced. Therefore, the number of design variables decreases from 64 to 16. The representation of stacking sequence of 64 layered composite plate can be given as

$$[\pm\theta_1 / \pm\theta_2 / \pm\theta_3 / \pm\theta_4 / \pm\theta_5 / \pm\theta_6 / \pm\theta_7 / \pm\theta_8 / \pm\theta_9 / \pm\theta_{10} / \pm\theta_{11} / \pm\theta_{12} / \pm\theta_{13} / \pm\theta_{14} / \pm\theta_{15} / \pm\theta_{16}]_s$$

The mathematical representation of the optimization problem for this thesis can be stated as

Find: $\{\theta_k\},\ \theta_k \in \{-90,90\},\ k = 1,...,n$

Maximize: Critical buckling load factor (λ_{cb})

Subject to: The first ply failure (Puck failure criterion)

Prior to obtaining the optimum designs of composite plates, verification of algorithms, buckling load factor and Puck failure criterion has been carried out using specific results from previous studies in the literature. The critical buckling load factor (λ_{cb}) has been used as an objective function in optimization. The objective function for each design has been obtained using the MATLAB *Symbolic Math Toolbox* and the algorithm is given in Appendix A. Here, the smallest value within λ_b (1, 1), λ_b(1, 2), λ_b(2, 1) and λ_b(2, 2) has been taken as the critical buckling load factor (λ_{cb}). These specific objective functions have been maximized in optimization process. Having obtained maximized critical buckling load factor, the convenience of the designs in terms of Puck failure criterion has been tested layer by layer. In order to show the advantage of using continuous fiber angles in stacking sequence designs, continuous designs and discrete designs whose fiber angles are conventional (0, ±45, 90) for a/b = 2 and a/b = 1/2 plate aspect ratios have been compared. Additionally, the optimum designs of 48 layered composite plate with the same material and plate dimensions have been investigated for N_x = 3000 N/mm and the results have been compared with 64-layered plate designs. A comparison of Puck and Tsai-Wu failure criteria efforts for specific designs has also been performed. Finally, the investigation of optimum designs for N_x = 3000 N/mm loading considering Puck inter-fiber failure mode C (IFFC) have been studied.

6.2. Optimization Results and Evaluation

In the thesis study, the laminated composite plates subjected to in-plane loads have been analyzed using Genetic Algorithm optimization method in MATLAB *Global Optimization Toolbox* for the given load ratios and plate aspect ratios. The optimum

stacking sequence designs have been investigated considering buckling and failure criteria. In order to increase efficiency and reliability of GA, i) 50 independent searches have been performed for each case, ii) each of them has been stopped after 1000 function evaluations and iii) GA Toolbox options have been adjusted as in Table 5.1.

Firstly, in order to indicate that the optimization algorithms are reliable, the algorithms related to objective function (critical buckling load factor) and Puck failure criterion have been verified using some convenient results from previous studies in the literature. The results of buckling load factor algorithm verification for loading cases (LC1-LC9) specified in the study of Karakaya and Soykasap (2009) are given in Table 6.3. Similarly, the results of Puck failure criterion algorithm are given in Table 6.4.

Table 6.3. Verification of objective function algorithm

Loading Cases	**λ_{cb} (Karakaya and Soykasap 2009)**	**λ_{cb} (Present Study)**
LC1	695,781.30	695,663.1
LC2	242,823.10	242,844.4
LC3	173,945.30	173,915.8
LC4	1,057,948.30	1,057,902.7
LC5	323,764.00	323,792.5
LC6	206492.9	206,518.0
LC7	412,985.80	413,036.0
LC8	161,882.10	161,896.2
LC9	132,243.50	132,237.8

In Table 6.3, it has been found that the critical buckling load factor values are close to the values given by Karakaya and Soykasap (2009). This means that the present buckling load factor algorithm could yield reliable results.

Table 6.4 shows the comparison between the study of Lopez et al. (2009) and the present work for Puck fiber failure effort obtained for specific plate geometry, material properties and loading cases. It can be observed that failure effort values are very close to each other. It should be noted in the table that PFC_fw denotes Puck failure criterion including weakening factor. It is understood from here that the failure program used in the study could also yield reliable results.

Table 6.4. Verification of Puck failure criterion algorithm

N_{xy}	Failure Criteria	f_E (Lopez, et al. 2009)	f_E (Present Study)
0	PFC	0.96	0.9634
	PFC_fw	0.96	0.9634
100	PFC	0.98	0.9817
	PFC_fw	0.98	0.9817
250	PFC	1.00	1.0095
	PFC_fw	1.00	1.0095
500	PFC	1.00	0.9975
	PFC_fw	1.00	0.9975
1000	PFC	0.98	0.9798
	PFC_fw	0.98	0.9798

The optimum composite plate designs which resist to buckling and ply failure, and failed designs (shown in grey color) which are buckled or failed due to Puck failure criterion for various plate aspect ratios are given in Tables 6.5 - 6.8. The plate aspect ratios considered are a/b = 1, 2, 4 and 1/2. In all the tables, maximized critical buckling load factors (λ_{cb}), stacking sequences, failure efforts ($f_{E(FF)}$ and $f_{E(IFF)}$) and critical layer numbers (LN_{cr}) have been presented as optimization results.

Table 6.5 shows the optimum designs of laminated composite plates for the plate aspect ratio a/b = 1. It can be observed that all possible fiber orientations consist of combinations of +45 or -45 angles which are discrete values. Reliable plate designs in terms of buckling and ply failure have been obtained only for N_x = 1000 N/mm load, however, they have not been achieved for N_x = 3000 N/mm, 5000 N/mm and 10000 N/mm loads. Failure effort values of the optimum designs indicate that the optimum designs are safe in terms of the first ply failure (f_E >1). As seen, buckled (or failed) designs of composite plates are also given so as to point out that they are bad designs. Therefore, the failure effort values of bad designs have not been calculated.

Table 6.5. Optimum designs and corresponding failure efforts for $a/b = 1$

N_x (N/mm)	N_x/N_y	λ_{cb}	Stacking Sequence	$f_{E(FF)}$	LN_{cr}	$f_{E(IFF)}$	LN_{cr}
1000	1	1.63011	$[\mp 45/\pm 45/\mp 45_2/\pm 45/\mp 45_2/\pm 45/\mp 45/\pm 45_2/\mp 45/\pm 45_2/\mp 45_2]_s$	0.0699	27	5.10^{-8}	27
	2	2.17348	$[\mp 45/\pm 45/\mp 45_2/\pm 45/\mp 45/\pm 45_2/\mp 45/\pm 45/\mp 45/\pm 45_2/\mp 45_2/\pm 45_2]_s$	0.0538	31	0.1329	31
	4	2.60817	$[\pm 45/\mp 45/\pm 45_2/\mp 45/\pm 45_3/\mp 45_4/\pm 45/\mp 45_3]_s$	0.0441	31	0.2096	32
	1/2	1.08674	$[\pm 45_2/\mp 45/\pm 45_2/\mp 45_2/\pm 45_3/\mp 45_3/\pm 45_3]_s$	0.1063	31	0.2658	31
3000	1	0.54337	$[\pm 45/\mp 45/\pm 45/\mp 45/\pm 45/\mp 45_4/\pm 45_5/\mp 45/\pm 45]_s$	-	-	-	-
	2	0.72449	$[\mp 45_2/\pm 45_3/\mp 45/\pm 45/\mp 45/\pm 45/\mp 45/\pm 45/\mp 45_2/\pm 45_2/\mp 45]_s$	-	-	-	-
	4	0.86939	$[\mp 45_2/(\pm 45/\mp 45)_2/(\mp 45/\pm 45)_2/\mp 45_5/\pm 45]_s$	-	-	-	-
	1/2	0.36225	$[(\pm 45/\mp 45)_2/\mp 45/(\mp 45/\pm 45)_3/\mp 45_4/\pm 45]_s$	-	-	-	-
5000	1	0.32602	$[\mp 45/\pm 45/(\pm 45/\mp 45)_3/(\mp 45_2/\pm 45)_2/\mp 45_2]_s$	-	-	-	-
	2	0.4347	$[\mp 45/\pm 45_3/\mp 45/\pm 45_3/\mp 45/\pm 45_2/(\mp 45/\pm 45)_2/\mp 43.4]_s$	-	-	-	-
	4	0.52163	$[\mp 45_2/\pm 45_3/(\mp 45/\pm 45)_2/\pm 45/\mp 45_2/\pm 45_4]_s$	-	-	-	-
	1/2	0.21735	$[\pm 45/\mp 45_3/\pm 45/\mp 45_2/\pm 45_3/(\mp 45/\pm 45)_2/\pm 45_2]_s$	-	-	-	-
10000	1	0.16301	$[(\pm 45/\mp 45)_2/\pm 45_2/\mp 45/\pm 45_3/\mp 45_5/\pm 45]_s$	-	-	-	-
	2	0.21735	$[\pm 45_{16}]_s$	-	-	-	-
	4	0.26082	$[\pm 45/\mp 45_7/\pm 45_3/\mp 45_3/\pm 45/\mp 45]_s$	-	-	-	-
	1/2	0.10867	$[(\mp 45_2/\pm 45)_2/\mp 45/\pm 45_2/\mp 45_2/\pm 45_2/\mp 45/\pm 45_2]_s$	-	-	-	-

Table 6.6 shows the optimum designs of laminated composites for the plate aspect ratio of 2. It can be seen that all stacking sequences have continuous fiber angles in this case. It can be noticed that buckling load capacity increases with loading ratio. When the applied load is increased, it is observed that the designs are failed due to buckling and/or ply strength. The designs subjected to N_x = 1000 N/mm, 3000 N/mm and 5000 N/mm loads usually resulted well but any optimum design could not be obtained for 10000 N/mm loading. It can also be seen that in general, the critical layers

according to Puck failure theory are close to mid-plane (e.g., 27, 29, 31). In addition, the design for N_x = 5000 N/mm and a/b = 1, which is a bad design, has been controlled according to Puck failure criterion in order to show that the first ply failure occurs as expected.

Table 6.6. Optimum designs and corresponding failure efforts for a/b = 2

N_x (N/mm)	N_x/N_y	λ_{cb}	Stacking Sequence	$f_{E(FF)}$	LN_{cr}	$f_{E(IFF)}$	LN_{cr}
1000	1	4.8486	$[\mp 71.7/\pm 74/\mp 70.4/\mp 67.5/\mp 71.1/\mp 72.5/\mp 70/\pm 70.6/\mp 70/\mp 68.5/\mp 69.4/\mp 70.1/\pm 67.2/\pm 50.3/\pm 74.9/\mp 86]_s$	0.188	28	0.079	27
	2	7.5370	$[\pm 62.7/\mp 61.7/\pm 62.8/\pm 61.8/\mp 62.3/\pm 62.5/\pm 61.2/\pm 62.5/\mp 63.3/\mp 62.3/\mp 61/\pm 60.2/\pm 56.9/\mp 70.1/\pm 55.5/\mp 89.9]_s$	0.109	31	0.100	29
	4	10.083	$[\mp 53.3/\mp 53.4/\pm 53.1/\mp 52.9/\pm 53.4/\mp 53.4/\mp 53.2/\pm 53.3/\mp 52.8_2/\pm 53.4/\mp 53.1/\mp 52.7/\pm 58.8/\mp 51.1/\pm 79.8]_s$	0.192	31	0.145	29
	1/2	2.7973	$[\pm 88.8/\pm 80.2/\mp 78.2/\mp 76.7/\mp 80.5/\mp 78.9/\mp 72.6/\mp 78.7/\pm 79.2/\pm 67.8/\mp 83/\mp 69.6/\pm 88.5/\mp 75.3/\mp 60.4/\pm 30.6]_s$	0.257	31	0.031	31
3000	1	1.6152	$[\mp 68.3/\pm 72/\pm 68.8/\mp 69.8/\pm 69.2/\pm 72.3/\mp 78/\pm 66.2/\pm 76.7/\mp 73.8/\pm 89.5/\mp 78.5/\mp 58.4/\mp 70.5/\pm 89.2/\pm 28]_s$	0.799	31	0.261	31
	2	2.5116	$[\pm 61.5/\mp 63.6/\mp 62.7/\pm 61.3/\pm 63.7/\mp 61.6/\mp 63.1/\pm 60.8/\mp 61.1/\pm 61.5/\mp 60.8/\pm 58/\mp 68/\pm 57.4/\pm 48.5/\pm 32]_s$	0.756	31	0.369	31
	4	3.3598	$[\pm 54.2/\mp 53.1/\pm 53.3/\mp 52.6/\pm 53.3/\mp 53.6/\pm 54.1/\pm 50.6/\pm 52/\mp 51.7/\mp 53.9/\pm 55/\mp 50.3/\mp 52.3/\pm 65.2/\pm 71.3]_s$	0.436	31	0.454	25
	1/2	0.9322	$[\mp 83.3/\mp 72.5/\mp 78.3/\mp 82.1/\mp 79.2/\pm 88.6/\mp 77.8/90_2/\mp 82.4/\mp 73.6/\pm 76.2/\pm 61.2/\pm 86.5/\mp 82.6/\pm 61.5/\pm 59.7]_s$	-	-	-	-

(cont. on next page)

Table 6.6 (Cont.)

5000	1	0.9685	$[\mp 68.9/\mp 66.5/\mp 79.3/\pm 71.6/\pm 71.4/\mp 73.2/\pm 70.6/\pm 65.9/\mp 67.5/\mp 67.7/\mp 77.9/\pm 89.2/\mp 69.5/\mp 78.9/\mp 39.4/\mp 25.6]_s$	1.1511	31	1.2308	31
	2	1.5071	$[\pm 62.3/\pm 61.9/\mp 62.8/\mp 61.3/\mp 62.8/\pm 61.3/\mp 62.7/\pm 62/\pm 63.5/\pm 61.2/\mp 60.9/\mp 57.9/\pm 64.1/\mp 86/\pm 69.7/\mp 87.7]_s$	0.4468	31	0.4373	23
	4	2.0155	$[\mp 52.5/\mp 53.6/\mp 53.1/\pm 54.2/\pm 54.3/\pm 54.1/\pm 51.3/\mp 53.1_2/\pm 54.6/\pm 54.1/\mp 49.4/\pm 50.4/\pm 47.1/\mp 42.3/\pm 67.1]_s$	0.8156	29	0.9954	29
	1/2	0.5592	$[\pm 89.5_2/\mp 78.1/\mp 71.1/\pm 82.7/\pm 72.3/\pm 76.3/\pm 89.8/\pm 81.9/\pm 69.2/\mp 79.8/\mp 69.1/\mp 71/\pm 76.6/\mp 77.2/\pm 60.4]_s$	-	-	-	-
10000	1	0.4842	$[\pm 75.5/\mp 71.1/\pm 69.6/\mp 68.7/\mp 76/\mp 66.5_2/\pm 65.7/\mp 83.7/\pm 66.9/\mp 65/\pm 83.1/\mp 58.1/\mp 63.7/\mp 64.6/\mp 3.2]_s$	-	-	-	-
	2	0.7504	$[\pm 62.9/\mp 66.8/\pm 61/\mp 66.8/\mp 61/\pm 62.5/\pm 59.5/\pm 58.3/\pm 57.8/\mp 64.2/\mp 52.1/\mp 51.2/\mp 46.2/\mp 48.1/\mp 10.8/\mp 60.2]_s$	-	-	-	-
	4	1.0073	$[\pm 52.7/\pm 54.5/\pm 54.2/\pm 53/\pm 55.7/\pm 52.8/\pm 53.5/\pm 51.1/\pm 51.2/\pm 52/\pm 51.4/\pm 48.9/\pm 48.2/\pm 44.7/\pm 38.8/\pm 33.6]_s$	2.082	31	36.036	31
	1/2	0.2796	$[\mp 79.8/\mp 81.6/\pm 89.8/\mp 71.8/\pm 87.4/\pm 75.4/\pm 86.1/\mp 77.9/\pm 77.5/\pm 72.2/\mp 63.1/\mp 81.7/\mp 69.5/\mp 76.7/\mp 77/\pm 42.2]_s$	-	-	-	-

Table 6.7 shows the optimum designs for the plate aspect ratio of 4. As seen in the table, all obtained designs are safe for both buckling and the first ply failure. Stacking sequences only consist of 90˚ discrete fiber angle. Again, it can be observed that buckling load capacity of designs increases when the load ratio increases. The critical cases here occurred in the plates subjected to N_x = 10000 N/mm load as expected.

Table 6.7. Optimum designs and corresponding failure efforts for $a/b = 4$

N_x (N/mm)	N_x/N_y	λ_{cb}	Stacking Sequence	$f_{E(FF)}$	LN_{cr}	$f_{E(IFF)}$	LN_{cr}
1000	1	20.5288	$[90_{32}]_s$	0.0329	27	2.10^{-9}	27
	2	34.2147	$[90_{32}]_s$	0.0137	27	2.10^{-9}	27
	4	51.3221	$[90_{32}]_s$	0.0041	3	1.10^{-8}	3
	1/2	11.4049	$[90_{32}]_s$	0.0711	17	9.10^{-8}	17
3000	1	6.8429	$[90_{32}]_s$	0.0986	13	1.10^{-6}	13
	2	11.4049	$[90_{32}]_s$	0.0412	29	2.10^{-8}	29
	4	17.1073	$[90_{32}]_s$	0.0124	31	2.10^{-9}	31
	1/2	3.8016	$[90_{32}]_s$	0.2134	21	6.10^{-5}	21
5000	1	4.1058	$[90_{32}]_s$	0.1643	31	2.10^{-5}	31
	2	6.8429	$[90_{32}]_s$	0.0686	9	4.10^{-7}	9
	4	10.2644	$[90_{32}]_s$	0.0207	29	6.10^{-9}	29
	1/2	2.2810	$[90_{32}]_s$	0.3557	11	0.0014	11
10000	1	2.0529	$[90_{32}]_s$	0.3286	31	0.0014	31
	2	3.4215	$[90_{32}]_s$	0.1372	23	2.10^{-5}	23
	4	5.1322	$[90_{32}]_s$	0.0414	29	4.10^{-7}	29
	1/2	1.1405	$[90_{32}]_s$	0.7115	31	0.0889	31

The optimum designs for the plate aspect ratio of 1/2 are given in Table 6.8. The optimum designs could be obtained only for 1000 N/mm loading cases. It can be seen from the results in the table that all stacking sequences have continuous fiber angles. It is interesting to note that for N_x = 1000 N/mm and N_x/N_y = 1/2 case, the stacking sequence of the design consists of 0 discrete angle merely. It can also be noted that the critical loads ($N_{x,cr}$, $N_{y,cr}$), which the plate could withstand to, are close to the applied loads in the obtained designs. Furthermore, in all cases, the critical buckling load factor values increase depending on the increase in loading ratios.

Table 6.8. Optimum designs and corresponding failure efforts for a/b = 1/2

N_x (N/mm)	N_x/N_y	λ_{cb}	Stacking Sequence	$f_{E(FF)}$	LN_{cr}	$f_{E(IFF)}$	LN_{cr}
1000	1	1.2101	$[\pm 21.3/\pm 23.4/\pm 18.6/\mp 20.5/\pm 8.7/\pm 26.5/\pm 11.3/\pm 17.8/\mp 19.7/\mp 14/\mp 10.6/\pm 3.5/\mp 14.1/\pm 34.2/\pm 7.2/\mp 42.4]_s$	0.1961	31	0.0709	31
	2	1.3995	$[\pm 12.7/\pm 8.5/\pm 8.3/\mp 11/\pm 9.1/\mp 14.6/\pm 10.8/\pm 11.2/\mp 16.5/\mp 13.3/\pm 10/\mp 16.2/\pm 10.4/\pm 10.3/\pm 10.6/\pm 7.7]_s$	0.0470	17	0.0093	17
	4	1.5095	$[0_{32}]_s$	0.0369	23	1.10^{-9}	23
	1/2	0.9385	$[\mp 29.8/\mp 26.5/\pm 28.9/\mp 28.4/\mp 28.7/\mp 29.1/\pm 29.2/\pm 32.4/\pm 2.9/\mp 27.5/\mp 33/\mp 5.1/\mp 29.8/\mp 9.8/\mp 57.1/\pm 68.2]_s$	-	-	-	-
3000	1	0.4032	$[\pm 17.9/\pm 25.7/\mp 23.4/\pm 19.4/\mp 11.1/\pm 5/\mp 20.1/\pm 19.3/\mp 7.4/\pm 24.9/\pm 20/\pm 21.9/\pm 19.7/\mp 35/\mp 19.3/\pm 48.8]_s$	-	-	-	-
	2	0.4662	$[\mp 14.5/\pm 4.9/\pm 12.6/\pm 11.3/\pm 11/\pm 10.5/\pm 9.9/\pm 8.6/\pm 10/\pm 6.8/\pm 5.9/\pm 28.5/\mp 10.5/\pm 4/\pm 36.2/\mp 38.9]_s$	-	-	-	-
	4	0.5032	$[0_{32}]_s$	-	-	-	-
	1/2	0.3135	$[\pm 25.9/\mp 27.8_2/\mp 24.5/\pm 28.2/\pm 29.2/\pm 31.8/\pm 31.6/\pm 25.1/\mp 28.2/\mp 34.3/\pm 39.2/\pm 27/\pm 16.2/\mp 7.4/\pm 65.8]_s$	-	-	-	-
5000	1	0.2420	$[\pm 23.3/\pm 21.2/\mp 19/\pm 16.7/\mp 11.7/\mp 22.1/\pm 9.6/\pm 27.9/\pm 10/\pm 25.7/\mp 14.8/\mp 15.8/\pm 12.2/\pm 6.5/\pm 10.7/\pm 1.5]_s$	-	-	-	-
	2	0.2798	$[\pm 13.4/\mp 16.5/\mp 12/\pm 12.4/\mp 8.1/\pm 5.2/\pm 2.4/\pm 8.1/\pm 7.9/\pm 2.9/\pm 3.8/\pm 4.2/\pm 8/\pm 1.4/\mp 31.2/\pm 7]_s$	-	-	-	-
	4	0.3019	$[0_{32}]_s$	-	-	-	-
	1/2	0.1873	$[\pm 31.9/\mp 28.6/\mp 26.1/\mp 29.8/\mp 31/\mp 24/\mp 24.2/\pm 17.9/\mp 27.9/\mp 31.2/\pm 31/\pm 6.4/\pm 7.6/\pm 80.1/\mp 37.6/\pm 89]_s$	-	-	-	-
10000	1	0.1211	$[\mp 21.1/\mp 17.2\pm 22.3/\pm 21.4/\pm 15.1/\mp 24.2/\pm 3.4/\mp 16.1/\pm 19/\mp 14.6/\mp 20.1/\mp 28.8_2/\pm 3.1/\pm 2.9/\pm 47.8]_s$	-	-	-	-
	2	0.1397	$[\mp 18.2/\pm 9.3/\pm 0.7/\mp 18.8/\pm 3.5/\pm 3.7/\pm 1.8/\pm 4.7/\mp 6.3/\pm 4.9/\pm 24.4/\pm 0.8/\pm 0.7/\mp 22.9/\pm 0.3/\mp 2.5]_s$	-	-	-	-
	4	0.1509	$[0_{32}]_s$	-	-	-	-
	1/2	0.0937	$[\mp 23.9/\pm 29.1/\mp 27.9/\mp 22.1/\pm 33.3/\mp 27.2/\mp 24.7/\mp 29.4/\mp 25.2/\pm 39.4/\pm 41.3/\mp 33.3/\mp 46.7/\pm 27.1/\pm 32.6/\mp 79.3]_s$	-	-	-	-

Eventually, it can be observed that the stacking sequences include both continuous and discrete fiber angles depending on the aspect ratios. As touched briefly in the previous discussions, stacking sequences hold continuous fiber angles in plate aspect ratios of 2 and 1/2 except a few special cases, and stacking sequences hold discrete fiber angles when the plate aspect ratios are 1 and 4. It can be noted from the tables that when the applied load is increased, maximized critical buckling load factor values decreases. In other words, the number of the optimum designs decreases so long as the applied load is increased.

In Tables 6.9 – 6.12, the effect of various plate aspect ratios on optimum laminated composite plate designs has been investigated depending on loading ratios. The tables have been generated for N_x = 1000 N/mm, 3000 N/mm, 5000 N/mm and 10000 N/mm loads. These tables also include optimum designs, maximized critical buckling load factors and the first ply failure efforts with corresponding critical layer numbers.

As seen in Table 6.9, an optimum laminated composite design has been found in almost all considered cases. The largest critical buckling load factor values have been obtained in the plates with aspect ratio of 4, which means that the related designs would be able to withstand further loading. In Table 6.10, it can be seen that the reliable optimum designs have been decreased depending on load raise, and this situation can be observed clearly in the other tables as well. In this loading case, there are seven reliable designs which are not buckled or failed. It can also be noted that the critical layers in terms of Puck failure criteria are mostly near the mid- plane of the laminates. Table 6.11 shows the optimum designs for N_x = 5000 N/mm load and only six reliable designs exist. It can be observed that the designed plates having 2 and 4 aspect ratios are more resistant than the others in terms of buckling and ply failure strength. Table 6.12 shows the results for the case of maximum applied loading. It can be seen that only four good designs resisting to buckling and the first ply failure could be obtained under this loading condition. The critical optimum design is the plate in the case of N_x/N_y = 1/2 and a/b = 1 because the critical buckling load factor almost equals to one.

Table 6.9. Optimum designs and corresponding failure efforts for N_x = 1000 N/mm

N_x/N_y	a/b	λ_{cb}	Stacking Sequence	$f_{E(FF)}$	LN_{cr}	$f_{E(IFF)}$	LN_{cr}
1	1	1.6301	$[\mp 45/(\pm 45/\mp 45_2)_2/\pm 45/\mp 45/\pm 45_2/\mp 45/\pm 45_2/\mp 45_2]_s$	0.0699	27	5.10^{-8}	27
	2	4.8486	$[\mp 71.7/\pm 74/\mp 70.4/\mp 67.5/\mp 71.1/\mp 72.5/\mp 70/\pm 70.6/\mp 70/\mp 68.5/\mp 69.4/\mp 70.1/\pm 67.2/\pm 50.3/\pm 74.9/\mp 86]_s$	0.188	28	0.0786	27
	4	20.529	$[90_{32}]_s$	0.0329	27	2.10^{-9}	27
	1/2	1.2101	$[\pm 21.3/\pm 23.4/\pm 18.6/\mp 20.5/\pm 8.7/\pm 26.5/\pm 11.3/\pm 17.8/\mp 19.7/\mp 14/\mp 10.6/\pm 3.5/\mp 14.1/\pm 34.2/\pm 7.2/\mp 42.4]_s$	0.1961	31	0.0709	31
2	1	2.1735	$[\mp 45/\pm 45/\mp 45_2/\pm 45/\mp 45/\pm 45_2/\mp 45/\pm 45/\mp 45/\pm 45_2/\mp 45_2/\pm 45_2]_s$	0.0538	31	0.1329	31
	2	7.537	$[\pm 62.7/\mp 61.7/\pm 62.8/\pm 61.8/\mp 62.3/\pm 62.5/\pm 61.2/\pm 62.5/\mp 63.3/\mp 62.3/\mp 61/\pm 60.2/\pm 56.9/\mp 70.1/\pm 55.5/\mp 89.9]_s$	0.1092	31	0.1006	29
	4	34.215	$[90_{32}]_s$	0.0137	27	2.10^{-10}	27
	1/2	1.3995	$[\pm 12.7/\pm 8.5/\pm 8.3/\mp 11/\pm 9.1/\mp 14.6/\pm 10.8/\pm 11.2/\mp 16.5/\mp 13.3/\pm 10/\mp 16.2/\pm 10.4/\pm 10.3/\pm 10.6/\pm 7.7]_s$	0.047	17	0.0093	17
4	1	2.6082	$[\pm 45/\mp 45/\pm 45_2/\mp 45/\pm 45_3/\mp 45_4/\pm 45/\mp 45_3]_s$	0.0441	31	0.2096	32
	2	10.083	$[\mp 53.3/\mp 53.4/\pm 53.1/\mp 52.9/\pm 53.4/\mp 53.4/\mp 53.2/\pm 53.3/\mp 52.8_2/\pm 53.4/\mp 53.1/\mp 52.7/\pm 58.8/\mp 51.1/\pm 79.8]_s$	0.1924	31	0.1454	29
	4	51.322	$[90_{32}]_s$	0.0041	3	1.10^{-8}	3
	1/2	1.5095	$[0_{32}]_s$	0.0369	23	1.10^{-9}	23
1/2	1	1.0867	$[\pm 45_2/\mp 45/\pm 45_2/\mp 45_2/\pm 45_3/\mp 45_3/\pm 45_3]_s$	0.1063	31	0.2658	31
	2	2.7972	$[\pm 88.8/\pm 80.2/\mp 78.2/\mp 76.7/\mp 80.5/\mp 78.9/\mp 72.6/\mp 78.7/\pm 79.2/\pm 67.8/\mp 83/\mp 69.6/\pm 88.5/\mp 75.3/\mp 60.4/\pm 30.6]_s$	0.257	31	0.0311	31
	4	11.405	$[90_{32}]_s$	0.0711	17	9.10^{-8}	17
	1/2	0.9385	$[\mp 29.8/\mp 26.5/\pm 28.9/\mp 28.4/\mp 28.7/\mp 29.1/\pm 29.2/\pm 32.4/\pm 2.9/\mp 27.5/\mp 33/\mp 5.1/\mp 29.8/\mp 9.8/\mp 57.1/\pm 68.2]_s$	-	-	-	-

Table 6.10. Optimum designs and corresponding failure efforts for N_x = 3000 N/mm

N_x/N_y	a/b	λ_{cb}	Stacking Sequence	$f_{E(FF)}$	LN_{cr}	$f_{E(IFF)}$	LN_{cr}
1	1	0.5434	$[\pm 45/\mp 45/\pm 45/\mp 45/\pm 45/\mp 45_4/\pm 45_5/\mp 45/\pm 45]_s$	-	-	-	-
	2	1.6152	$[\mp 68.3/\pm 72/\pm 68.8/\mp 69.8/\pm 69.2/\pm 72.3/\mp 78/\pm 66.2/\pm 76.7/\mp 73.8/\pm 89.5/\mp 78.5/\mp 58.4/\mp 70.5/\pm 89.2/\pm 28]_s$	0.7986	31	0.2609	31
	4	6.8429	$[90_{32}]_s$	0.0986	13	1.10^{-6}	13
	1/2	0.4032	$[\pm 17.9/\pm 25.7/\mp 23.4/\pm 19.4/\mp 11.1/\pm 5/\mp 20.1/\pm 19.3/\mp 7.4/\pm 24.9/\pm 20/\pm 21.9/\pm 19.7/\mp 35/\mp 19.3/\pm 48.8]_s$	-	-	-	-
2	1	0.7245	$[\mp 45_2/\pm 45_3/(\mp 45/\pm 45)_3/\mp 45_2/\pm 45_2/\mp 45]_s$	-	-	-	-
	2	2.5116	$[\pm 61.5/\mp 63.6/\mp 62.7/\pm 61.3/\pm 63.7/\mp 61.6/\mp 63.1/\pm 60.8/\mp 61.1/\pm 61.5/\mp 60.8/\pm 58/\mp 68/\pm 57.4/\pm 48.5/\pm 32]_s$	0.7559	31	0.3693	31
	4	11.405	$[90_{32}]_s$	0.0412	29	2.10^{-8}	29
	1/2	0.4662	$[\mp 14.5/\pm 4.9/\pm 12.6/\pm 11.3/\pm 11/\pm 10.5/\pm 9.9/\pm 8.6/\pm 10/\pm 6.8/\pm 5.9/\pm 28.5/\mp 10.5/\pm 4/\pm 36.2/\mp 38.9]_s$	-	-	-	-
4	1	0.8694	$[\mp 45_2/(\pm 45/\mp 45)_2/(\mp 45/\pm 45)_2/\mp 45_5/\pm 45]_s$	-	-	-	-
	2	3.3598	$[\pm 54.2/\mp 53.1/\pm 53.3/\mp 52.6/\pm 53.3/\mp 53.6/\pm 54.1/\pm 50.6/\pm 52/\mp 51.7/\mp 53.9/\pm 55/\mp 50.3/\mp 52.3/\pm 65.2/\pm 71.3]_s$	0.4359	31	0.4543	25
	4	17.107	$[90_{32}]_s$	0.0124	31	2.10^{-9}	31
	1/2	0.5032	$[0_{32}]_s$	-	-	-	-
1/2	1	0.3622	$[(\pm 45/\mp 45)_2/\mp 45/(\mp 45/\pm 45)_3/\mp 45_4/\pm 45]_s$	-	-	-	-
	2	0.9322	$[\mp 83.3/\mp 72.5/\mp 78.3/\mp 82.1/\mp 79.2/\pm 88.6/\mp 77.8/90_2/\mp 82.4/\mp 73.6/\pm 76.2/\pm 61.2/\pm 86.5/\mp 82.6/\pm 61.5/\pm 59.7]_s$	-	-	-	-
	4	3.8016	$[90_{32}]_s$	0.2134	21	6.10^{-5}	21
	1/2	0.3135	$[\pm 25.9/\mp 27.8_2/\mp 24.5/\pm 28.2/\pm 29.2/\pm 31.8/\pm 31.6/\pm 25.1/\mp 28.2/\mp 34.3/\pm 39.2/\pm 27/\pm 16.2/\mp 7.4/\pm 65.8]_s$	-	-	-	-

Table 6.11. Optimum designs and corresponding failure efforts for N_x = 5000 N/mm

N_x/N_y	a/b	λ_{cb}	Stacking Sequence	$f_{E(FF)}$	LN_{cr}	$f_{E(IFF)}$	LN_{cr}
1	1	0.326	$[\mp 45/\pm 45/(\pm 45/\mp 45)_3/(\mp 45_2/\pm 45)_2/\mp 45_2]_s$	-	-	-	-
	2	0.9685	$[\mp 68.9/\mp 66.5/\mp 79.3/\pm 71.6/\pm 71.4/\mp 73.2/\pm 70.6/\pm 65.9/\mp 67.5/\mp 67.7/\mp 77.9/\pm 89.2/\mp 69.5/\mp 78.9/\mp 39.4/\mp 25.6]_s$	1.1511	31	1.2308	31
	4	4.1058	$[90_{32}]_s$	0.1643	31	2.10^{-5}	31
	1/2	0.242	$[\pm 23.3/\pm 21.2/\mp 19/\pm 16.7/\mp 11.7/\mp 22.1/\pm 9.6/\pm 27.9/\pm 10/\pm 25.7/\mp 14.8/\mp 15.8/\pm 12.2/\pm 6.5/\pm 10.7/\pm 1.5]_s$	-	-	-	-
2	1	0.4347	$[\mp 45/\pm 45_3/\mp 45/\pm 45_3/\mp 45/\pm 45_2/(\mp 45/\pm 45)_2/\mp 43.4]_s$	-	-	-	-
	2	1.5071	$[\pm 62.3/\pm 61.9/\mp 62.8/\mp 61.3/\mp 62.8/\pm 61.3/\mp 62.7/\pm 62/\pm 63.5/\pm 61.2/\mp 60.9/\mp 57.9/\pm 64.1/\mp 86/\pm 69.7/\mp 87.7]_s$	0.4468	31	0.4373	23
	4	6.8429	$[90_{32}]_s$	0.0686	9	4.10^{-7}	9
	1/2	0.2798	$[\pm 13.4/\mp 16.5/\mp 12/\pm 12.4/\mp 8.1/\pm 5.2/\pm 2.4/\pm 8.1/\pm 7.9/\pm 2.9/\pm 3.8/\pm 4.2/\pm 8/\pm 1.4/\mp 31.2/\pm 7]_s$	-	-	-	-
4	1	0.5216	$[\mp 45_2/\pm 45_3/(\mp 45/\pm 45)_2/\pm 45/\mp 45_2/\pm 45_4]_s$	-	-	-	-
	2	2.0155	$[\mp 52.5/\mp 53.6/\mp 53.1/\pm 54.2/\pm 54.3/\pm 54.1/\pm 51.3/\mp 53.1_2/\pm 54.6/\pm 54.1/\mp 49.4/\pm 50.4/\pm 47.1/\mp 42.3/\pm 67.1]_s$	0.8156	29	0.9954	29
	4	10.264	$[90_{32}]_s$	0.0207	29	6.10^{-9}	29
	1/2	0.3019	$[0_{32}]_s$	-	-	-	-
1/2	1	0.2173	$[\pm 45/\mp 45_3/\pm 45/\mp 45_2/\pm 45_3/(\mp 45/\pm 45)_2/\pm 45_2]_s$	-	-	-	-
	2	0.5592	$[\pm 89.5_2/\mp 78.1/\mp 71.1/\pm 82.7/\pm 72.3/\pm 76.3/\pm 89.8/\pm 81.9/\pm 69.2/\mp 79.8/\mp 69.1/\mp 71/\pm 76.6/\mp 77.2/\pm 60.4]_s$	-	-	-	-
	4	2.281	$[90_{32}]_s$	0.3557	11	0.0014	11
	1/2	0.1873	$[\pm 31.9/\mp 28.6/\mp 26.1/\mp 29.8/\mp 31/\mp 24/\mp 24.2/\pm 17.9/\mp 27.9/\mp 31.2/\pm 31/\pm 6.4/\pm 7.6/\pm 80.1/\mp 37.6/\pm 89]_s$	-	-	-	-

Table 6.12. Optimum designs and corresponding failure efforts for N_x = 10000 N/mm

N_x/N_y	a/b	λ_{cb}	Stacking Sequence	$f_{E(FF)}$	LN_{cr}	$f_{E(IFF)}$	LN_{cr}
1	1	0.163	$[(\pm 45/\mp 45)_2/\pm 45_2/\mp 45/\pm 45_3/\mp 45_5/\pm 45]_s$	-	-	-	-
	2	0.4842	$[\pm 75.5/\mp 71.1/\pm 69.6/\mp 68.7/\mp 76/\mp 66.5_2/\pm 65.7/\mp 83.7/\pm 66.9/\mp 65/\pm 83.1/\mp 58.1/\mp 63.7/\mp 64.6/\mp 3.2]_s$	-	-	-	-
	4	2.0529	$[90_{32}]_s$	0.3286	31	0.0014	31
	1/2	0.1211	$[\mp 21.1/\mp 17.2\pm 22.3/\pm 21.4/\pm 15.1/\mp 24.2/\pm 3.4/\mp 16.1/\pm 19/\mp 14.6/\mp 20.1/\mp 28.8_2/\pm 3.1/\pm 2.9/\pm 47.8]_s$	-	-	-	-
2	1	0.2173	$[\mp 45/\pm 45/\mp 45_2/\pm 45_4/\mp 45/\pm 45/(\mp 45_2/\pm 45)_2]_s$	-	-	-	-
	2	0.7504	$[\pm 62.9/\mp 66.8/\pm 61/\mp 66.8/\mp 61/\pm 62.5/\pm 59.5/\pm 58.3/\pm 57.8/\mp 64.2/\mp 52.1/\mp 51.2/\mp 46.2/\mp 48.1/\mp 10.8/\mp 60.2]_s$	-	-	-	-
	4	3.4215	$[90_{32}]_s$	0.1372	23	2.10^{-5}	23
	1/2	0.1397	$[\mp 18.2/\pm 9.3/\pm 0.7/\mp 18.8/\pm 3.5/\pm 3.7/\pm 1.8/\pm 4.7/\mp 6.3/\pm 4.9/\pm 24.4/\pm 0.8/\pm 0.7/\mp 22.9/\pm 0.3/\mp 2.5]_s$	-	-	-	-
4	1	0.2608	$[\pm 45/\mp 45_7/\pm 45_3/\mp 45_3/\pm 45/\mp 45]_s$	-	-	-	-
	2	1.0073	$[\pm 52.7/\pm 54.5/\pm 54.2/\pm 53/\pm 55.7/\pm 52.8/\pm 53.5/\pm 51.1/\pm 51.2/\pm 52/\pm 51.4/\pm 48.9/\pm 48.2/\pm 44.7/\pm 38.8/\pm 33.6]_s$	2.082	31	36.036	31
	4	5.1322	$[90_{32}]_s$	0.0414	29	4.10^{-7}	29
	1/2	0.1509	$[0_{32}]_s$	-	-	-	-
1/2	1	0.1087	$[(\mp 45_2/\pm 45)_2/\mp 45/\pm 45_2/\mp 45_2/\pm 45_2/\mp 45/\pm 45_2]_s$	-	-	-	-
	2	0.2796	$[\mp 79.8/\mp 81.6/\pm 89.8/\mp 71.8/\pm 87.4/\pm 75.4/\pm 86.1/\mp 77.9/\pm 77.5/\pm 72.2/\mp 63.1/\mp 81.7/\mp 69.5/\mp 76.7/\mp 77/\pm 42.2]_s$	-	-	-	-
	4	1.1405	$[90_{32}]_s$	0.7115	31	0.0889	31
	1/2	0.0937	$[\mp 23.9/\pm 29.1/\mp 27.9/\mp 22.1/\pm 33.3/\mp 27.2/\mp 24.7/\mp 29.4/\mp 25.2/\pm 39.4/\pm 41.3/\mp 33.3/\mp 46.7/\pm 27.1/\pm 32.6/\mp 79.3]_s$	-	-	-	-

In the thesis, fiber angles in the stacking sequences of the laminated composites have been assumed continuous and the optimization has been carried out considering this assumption. However, discrete ply orientations are used by industry in design of laminated composite materials due to their economic production methods. In order to

indicate that the advantages of studying with continuous design variables (fiber angles), the stacking sequences (continuous case) of some optimum designs have been converted to designs including discrete fiber orientations and they have been presented together in Table 6.13 and 6.14. These fiber angles have been converted into discrete variables by dividing the range into equal interval and specifying them to discrete values. 0˚, ±45˚ and 90˚ have been considered as three discrete angles. A continuous value between -90 and -30 has been specified as a discrete value of 0, a value between -30 and 30 has been specified as a discrete value of 45 and a value between 30 and 90 has been specified as a discrete value of 90 in conversion process. It should be noted that since the plies are considered as ± stacks in order to provide the balance of the laminate; so 0, 45 and 90 fiber angles are used as 0_2, ±45, 90_2 respectively in the stacking sequences.

Table 6.13 represents the comparison of the optimum continuous stacking sequence designs and their converted ones for the plate aspect ratio a/b = 2. Loadings, loading ratios, type of ply orientations, critical buckling load factors, stacking sequences, Puck fiber and inter-fiber failure efforts and their critical layer numbers are given in the table. The bad designs which failed due to buckling have not been converted. It can be seen from the table that all the converted designs for 1000 N/mm, 3000 N/mm and 5000 N/mm loads are also reliable according to buckling and the first ply failure. The optimum continuous designs for 10000 N/mm load have not been considered since there is not any reliable design in this case. It is obvious that in all cases, critical buckling load factor values show a decrease and converted stacking sequence designs therefore become weaker than the continuous ones. In other words, they are less resistant to withstand buckling.

Table 6.14 shows the comparison of optimum continuous stacking sequences at the plate aspect ratio of 1/2 for 1000 N/mm load considering Table 6.8 and their converted ones. The designs for the loads 3000 N/mm, 5000 N/mm and 10000 N/mm have not been considered since they did not give optimum results for the cases given in Table 6.8. It can clearly be seen from the table that the critical buckling load factor values decrease in all cases. There is only one reliable case which is the load ratio of 4 after the conversion.

As a conclusion, the comparison between the results obtained for both continuous and discrete (conventional) fiber orientations indicates that optimum critical buckling load factor value is higher when continuous orientations are used.

Table 6.13. Comparison of continuous (Cont) and discrete (Disc) optimum designs for $a/b = 2$

N_x	N_x/N_y	Type	λ_{cb}	Stacking Sequence	$f_{E(FF)}$	LN_{cr}	$f_{E(IFF)}$	LN_{cr}
1000	1	Cont	4.849	$[\mp 71.7/\pm 74/\mp 70.4/\mp 67.5/\mp 71.1/\mp 72.5/\mp 70/\pm 70.6/\mp 70/\mp 68.5/\mp 69.4/\mp 70.1/\pm 67.2/\pm 50.3/\pm 74.9/\mp 86]_s$	0.188	28	0.079	27
		Disc	1.799	$[0_2/90_2/0_{10}/90_2/0_8/90_6/0_2]_s$	0.105	3	6.10^{-7}	3
	2	Cont	7.537	$[\pm 62.7/\mp 61.7/\pm 62.8/\pm 61.8/\mp 62.3/\pm 62.5/\pm 61.2/\pm 62.5/\mp 63.3/\mp 62.3/\mp 61/\pm 60.2/\pm 56.9/\mp 70.1/\pm 55.5/\mp 89.9]_s$	0.109	31	0.101	29
		Disc	5.073	$[90_2/0_2/90_4/0_2/90_6/0_6/90_4/0_2/90_2/0_2]_s$	0.079	3	1.10^{-7}	3
	4	Cont	10.083	$[\mp 53.3/\mp 53.4/\pm 53.1/\mp 52.9/\pm 53.4/\mp 53.4/\mp 53.2/\pm 53.3/\mp 52.8_2/\pm 53.4/\mp 53.1/\mp 52.7/\pm 58.8/\mp 51.1/\pm 79.8]_s$	0.192	31	0.145	29
		Disc	5.442	$[0_2/(0_2/90_2)_2/(0_4/90_2)_3/0_2/90_2]_s$	0.058	1	2.10^{-8}	1
	1/2	Cont	2.797	$[\pm 88.8/\pm 80.2/\mp 78.2/\mp 76.7/\mp 80.5/\mp 78.9/\mp 72.6/\mp 78.7/\pm 79.2/\pm 67.8/\mp 83/\mp 69.6/\pm 88.5/\mp 75.3/\mp 60.4/\pm 30.6]_s$	0.257	31	0.031	31
		Disc	1.450	$[90_4/0_{12}/90_4/(0_4/90_2)_2]_s$	0.181	1	2.10^{-5}	1
3000	1	Cont	1.615	$[\mp 68.3/\pm 72/\pm 68.8/\mp 69.8/\pm 69.2/\pm 72.3/\mp 78/\pm 66.2/\pm 76.7/\mp 73.8/\pm 89.5/\mp 78.5/\mp 58.4/\mp 70.5/\pm 89.2/\pm 28]_s$	0.799	31	0.261	31
		Disc	1.116	$[(0_2/90_4)_3/0_2/90_2/0_6/90_2/\pm 45]_s$	0.223	1	4.10^{-4}	32
	2	Cont	2.512	$[\pm 61.5/\mp 63.6/\mp 62.7/\pm 61.3/\pm 63.7/\mp 61.6/\mp 63.1/\pm 60.8/\mp 61.1/\pm 61.5/\mp 60.8/\pm 58/\mp 68/\pm 57.4/\pm 48.5/\pm 32]_s$	0.756	31	0.369	31
		Disc	1.644	$[90_2/0_4/90_4/0_2/(0_2/90_2)_4/90_4]_s$	0.238	3	8.10^{-5}	3
	4	Cont	3.359	$[\pm 54.2/\mp 53.1/\pm 53.3/\mp 52.6/\pm 53.3/\mp 53.6/\pm 54.1/\pm 50.6/\pm 52/\mp 51.7/\mp 53.9/\pm 55/\mp 50.3/\mp 52.3/\pm 65.2/\pm 71.3]_s$	0.436	31	0.454	25
		Disc	2.029	$[(90_2/0_2)_3/90_4/(90_2/0_4)_2/90_4]_s$	0.240	3	9.10^{-5}	3
	1/2	Cont	0.932	$[\mp 83.3/\mp 72.5/\mp 78.3/\mp 82.1/\mp 79.2/\pm 88.6/\mp 77.8/90_2/\mp 82.4/\mp 73.6/\pm 76.2/\pm 61.2/\pm 86.5/\mp 82.6/\pm 61.5/\pm 59.7]_s$	0.466	32	0.126	31
		Disc	-	-	-	-	-	-

(cont. on next page)

Table 6.13 (Cont.)

5000	1	Cont	0.968	$[\mp 68.9/\mp 66.5/\mp 79.3/\pm 71.6/\pm 71.4/\mp 73.2/\pm 70.6/\pm 65.9/\mp 67.5/\mp 67.7/\mp 77.9/\pm 89.2/\mp 69.5/\mp 78.9/\mp 39.4/\mp 25.6]_s$	1.151	31	1.231	31
		Disc	-	-	-	-	-	-
	2	Con.	1.507	$[\pm 62.3/\pm 61.9/\mp 62.8/\mp 61.3/\mp 62.8/\pm 61.3/\mp 62.7/\pm 62/\pm 63.5/\pm 61.2/\mp 60.9/\mp 57.9/\pm 64.1/\mp 86/\pm 69.7/\mp 87.7]_s$	0.447	31	0.437	23
		Disc	1.015	$[90_4/0_6/90_2/0_2/90_6/0_4/(90_2/0_2)_2]_s$	0.354	5	9.10^{-4}	5
	4	Cont	2.015	$[\mp 52.5/\mp 53.6/\mp 53.1/\pm 54.2/\pm 54.3/\pm 54.1/\pm 51.3/\mp 53.1_2/\pm 54.6/\pm 54.1/\mp 49.4/\pm 50.4/\pm 47.1/\mp 42.3/\pm 67.1]_s$	0.816	29	0.995	29
		Disc	1.217	$[0_6/90_8/0_2/(0_2/90_4)_2/0_2/90_2]_s$	0.400	1	0.002	1
	1/2	Cont	0.559	$[\pm 89.5_2/\mp 78.1/\mp 71.1/\pm 82.7/\pm 72.3/\pm 76.3/\pm 89.8/\pm 81.9/\pm 69.2/\mp 79.8/\mp 69.1/\mp 71/\pm 76.6/\mp 77.2/\pm 60.4]_s$	-	-	-	-
		Disc	-	-	-	-	-	-
10000	1	Cont	0.484	$[\pm 75.5/\mp 71.1/\pm 69.6/\mp 68.7/\mp 76/\mp 66.5_2/\pm 65.7/\mp 83.7/\pm 66.9/\mp 65/\pm 83.1/\mp 58.1/\mp 63.7/\mp 64.6/\mp 3.2]_s$	-	-	-	-
		Disc	-	-	-	-	-	-
	2	Cont.	0.750	$[\pm 62.9/\mp 66.8/\pm 61/\mp 66.8/\mp 61/\pm 62.5/\pm 59.5/\pm 58.3/\pm 57.8/\mp 64.2/\mp 52.1/\mp 51.2/\mp 46.2/\mp 48.1/\mp 10.8/\mp 60.2]_s$	-	-	-	-
		Disc	-	-	-	-	-	-
	4	Cont	1.007	$[\pm 52.7/\pm 54.5/\pm 54.2/\pm 53/\pm 55.7/\pm 52.8/\pm 53.5/\pm 51.1/\pm 51.2/\pm 52/\pm 51.4/\pm 48.9/\pm 48.2/\pm 44.7/\pm 38.8/\pm 33.6]_s$	2.082	31	36.04	31
		Disc	0.609	$[90_{32}]_s$	-	-	-	-
	1/2	Cont	0.279	$[\mp 79.8/\mp 81.6/\pm 89.8/\mp 71.8/\pm 87.4/\pm 75.4/\pm 86.1/\mp 77.9/\pm 77.5/\pm 72.2/\mp 63.1/\mp 81.7/\mp 69.5/\mp 76.7/\mp 77/\pm 42.2]_s$	-	-	-	-
		Disc	-	-	-	-	-	-

Table 6.14. Comparison of continuous and discrete optimum designs for a/b = 1/2

N_x (N/mm)	N_x/N_y	Type	λ_{cb}	Stacking Sequence	$f_{E(FF)}$	LN_{cr}	$f_{E(IFF)}$	LN_{cr}
1000	1	Cont	1.2101	$[\pm 21.3/\pm 23.4/\pm 18.6/\mp 20.5/\pm 8.7/\pm 26.5/\pm 11.3/\pm 17.8/\mp 19.7/\mp 14/\mp 10.6/\pm 3.5/\mp 14.1/\pm 34.2/\pm 7.2/\mp 42.4]_s$	0.196	31	0.071	31
		Disc	0.8631	$[\pm 45_{26}/90_2/\pm 45/0_2]_s$	-	-	-	-
	2	Cont	1.3995	$[\pm 12.7/\pm 8.5/\pm 8.3/\mp 11/\pm 9.1/\mp 14.6/\pm 10.8/\pm 11.2/\mp 16.5/\mp 13.3/\pm 10/\mp 16.2/\pm 10.4/\pm 10.3/\pm 10.6/\pm 7.7]_s$	0.047	17	0.009	17
		Disc	0.9623	$[\pm 45_{32}]_s$	-	-	-	-
	4	Cont	1.5095	$[0_{32}]_s$	0.037	23	1.10^{-9}	23
		Disc	1.0189	$[\pm 45_{32}]_s$	0.047	1	0.201	1
	1/2	Cont	0.9385	$[\mp 29.8/\mp 26.5/\pm 28.9/\mp 28.4/\mp 28.7/\mp 29.1/\pm 29.2/\pm 32.4/\pm 2.9/\mp 27.5/\mp 33/\mp 5.1/\mp 29.8/\mp 9.8/\mp 57.1/\pm 68.2]_s$	-	-	-	-
		Disc	-	-	-	-	-	-

In addition to the investigation for optimum designs of 64-layered composite plates given in Tables 6.5 -6.12, 48-layered composite plates have also been considered.

In Table 6.15, the optimum designs of 48-layered composite plates for 3000 N/mm load are given. It can be observed that the number of reliable designs in terms of buckling and the first ply failure, and the values of critical buckling load factor decrease as compared to 64-layered design cases as expected. On the other hand, the obtained optimum designs of 48-layered composite plates could resist to the same loading conditions and they are lighter, which meets the requirements of industry.

Table 6.15. Optimum designs of 48-layered plates for N_x = 3000 N/mm

N_x/N_y	a/b	λ_{cb}	Stacking Sequence	$f_{E(FF)}$	LN_{cr}	$f_{E(IFF)}$	LN_{cr}
1	1	0.2292	$[(\mp 45_2 / \pm 45)_4]_s$	-	-	-	-
	2	0.6816	$[\mp 72.1 / \mp 68.9 / \mp 72.8 / \pm 71 / \pm 74.4 / \pm 68.7 / \mp 62.4 / \pm 71.6 / \pm 65.2 / \pm 89.8 / \pm 83 / \pm 56.4]_s$	-	-	-	-
	4	2.8869	$[90_{24}]_s$	0.1314	15	6.10^{-6}	15
	1/2	0.1704	$[\mp 16 / \pm 15.5 / \pm 22.3 / \mp 23.5 / \pm 18.1 / \pm 24.2 / \mp 21.4 / \pm 16.7 / \mp 15.2 / \pm 21.2 / \mp 26.2 / \mp 26.4]_s$	-	-	-	-
2	1	0.3056	$[\pm 45_4 / \mp 45_2 / \pm 45 / \mp 45 / \pm 45_4]_s$	-	-	-	-
	2	1.0588	$[\pm 62.9 / \mp 58.7 / \mp 62.1 / \pm 61.7 / \mp 63.9 / \mp 65.9 / \mp 62.6 / \pm 60.7 / \pm 64.1 / \pm 78.4 / \pm 59.6 / \mp 61.5]_s$	0.3372	19	0.3746	3
	4	4.8114	$[90_{24}]_s$	0.0549	7	9.10^{-8}	7
	1/2	0.1968	$[\pm 12.1 / \mp 13.2 / \pm 11.1 / \pm 10.3 / \pm 11.5 / \pm 10.8 / \pm 6.6 / \pm 7.1 / \pm 6.7 / \pm 4.9 / \pm 3.3 / \pm 5.1]_s$	-	-	-	-
4	1	0.3668	$[\mp 45 / \pm 45_2 / \mp 45 / \pm 45 / \mp 45_3 / (\pm 45 / \mp 45)_2]_s$	-	-	-	-
	2	1.417	$[\pm 52 / \pm 53.6 / \mp 52.3 / \mp 53.4 / \mp 54.9 / \mp 53.6 / \mp 54.1 / \mp 56.1 / \mp 56.2 / \pm 45.4 / \mp 52.8 / \pm 48.4]_s$	0.5431	19	0.7875	19
	4	7.2172	$[90_{24}]_s$	0.0166	23	1.10^{-9}	23
	1/2	0.2123	$[0_{24}]_s$	-	-	-	-
1/2	1	0.1528	$[(\pm 45 / \mp 45)_3 / \pm 45_2 / \mp 45_4]_s$	-	-	-	-
	2	0.3935	$[\mp 87.9 / \pm 74.4 / \mp 78.6 / \mp 77.8 / \mp 74.9 / \mp 80.7 / \pm 84.4 / \pm 73.5 / \mp 85.6 / \pm 82.1 / \pm 78.5 / \mp 72.7]_s$	-	-	-	-
	4	1.6038	$[90_{24}]_s$	0.2846	1	0.0004	1
	1/2	0.1323	$[\mp 27.6 / \mp 27.1 / \pm 26.2 / \mp 29.2 / \mp 26.7 / \pm 32 / \mp 25.5 / \mp 23.6 / \mp 32.7 / \mp 43.7 / \pm 45 / \mp 39.2]_s$	-	-	-	-

As another effort in the thesis, a comparative study of Puck and Tsai-Wu failure criteria has been performed so as to search for the reliability of the optimum designs in terms of Tsai-Wu failure criterion, and show the advantages of Puck failure criteria if exists. The results of the study are given in Table 6.16. As seen from the table, the critical optimum designs in terms of buckling have been considered. The load in the x direction, load ratio, plate aspect ratio, buckling load factor, stacking sequence; Puck fiber failure effort, Puck inter-fiber failure effort, Tsai-Wu failure effort and their critical layer numbers appear in the table.

In discussion of results, it has been observed that the half of designs is not reliable according to Tsai-Wu failure criterion; however, all the designs except one are reliable according to Puck failure criteria. This situation means that the optimum

designs resisting to buckling and the first ply failure could exist in fact if Puck failure criterion is considered.

Table 6.16. Comparison of Puck and Tsai-Wu failure theories for specific designs

N_x	N_x/N_y	a/b	λ_{cb}	Stacking Sequence	$f_{E(FF)}$	LN_{cr}	$f_{E(IFF)}$	LN_{cr}	$f_{E(TW)}$	LN_{cr}
1000	1	1/2	1.210	$[\pm 21.3/\pm 23.4/\pm 18.6/\mp 20.5/\pm 8.7/\pm 26.5/\pm 11.3/\pm 17.8/\mp 19.7/\mp 14/\mp 10.6/\pm 3.5/\mp 14.1/\pm 34.2/\pm 7.2/\mp 42.4]_s$	0.196	31	0.071	31	0.118	31
	2	1/2	1.399	$[\pm 12.7/\pm 8.5/\pm 8.3/\mp 11/\pm 9.1/\mp 14.6/\pm 10.8/\pm 11.2/\mp 16.5/\mp 13.3/\pm 10/\mp 16.2/\pm 10.4/\pm 10.3/\pm 10.6/\pm 7.7]_s$	0.047	17	0.009	17	0.138	17
	4	1/2	1.509	$[0_{32}]_s$	0.037	23	1.10^{-9}	23	0.093	23
	1/2	1	1.087	$[\pm 45_2/\mp 45/\pm 45_2/\mp 45_2/\pm 45_3/\mp 45_3/\pm 45_3]_s$	0.106	31	0.266	31	0.014	31
3000	1	2	1.615	$[\mp 68.3/\pm 72/\pm 68.8/\mp 69.8/\pm 69.2/\pm 72.3/\mp 78/\pm 66.2/\pm 76.7/\mp 73.8/\pm 89.5/\mp 78.5/\mp 58.4/\mp 70.5/\pm 89.2/\pm 28]_s$	0.799	31	0.261	31	0.291	21
	2	2	2.512	$[\pm 61.5/\mp 63.6/\mp 62.7/\pm 61.3/\pm 63.7/\mp 61.6/\mp 63.1/\pm 60.8/\mp 61.1/\pm 61.5/\mp 60.8/\pm 58/\mp 68/\pm 57.4/\pm 48.5/\pm 32]_s$	0.756	31	0.369	31	0.324	26
	4	2	3.360	$[\pm 54.2/\mp 53.1/\pm 53.3/\mp 52.6/\pm 53.3/\mp 53.6/\pm 54.1/\pm 50.6/\pm 52/\mp 51.7/\mp 53.9/\pm 55/\mp 50.3/\mp 52.3/\pm 65.2/\pm 71.3]_s$	0.436	31	0.454	25	1.291	31
	1/2	4	3.802	$[90_{32}]_s$	0.213	21	6.10^{-5}	21	1.632	3
5000	1	4	4.106	$[90_{32}]_s$	0.164	31	2.10^{-5}	31	6.471	15
	2	2	1.507	$[\pm 62.3/\pm 61.9/\mp 62.8/\mp 61.3/\mp 62.8/\pm 61.3/\mp 62.7/\pm 62/\pm 63.5/\pm 61.2/\mp 60.9/\mp 57.9/\pm 64.1/\mp 86/\pm 69.7/\mp 87.7]_s$	0.447	31	0.437	23	5.934	31
	4	2	2.016	$[\mp 52.5/\mp 53.6/\mp 53.1/\pm 54.2/\pm 54.3/\pm 54.1/\pm 51.3/\mp 53.1_2/\pm 54.6/\pm 54.1/\mp 49.4/\pm 50.4/\pm 47.1/\mp 42.3/\pm 67.1]_s$	0.816	29	0.995	29	3.666	31
	1/2	4	2.281	$[90_{32}]_s$	0.356	11	0.001	11	6.078	21
10000	1	4	2.053	$[90_{32}]_s$	0.329	31	0.001	31	30.58	5
	2	4	3.421	$[90_{32}]_s$	0.137	23	2.10^{-5}	23	31.48	1
	4	2	1.007	$[\pm 52.7/\pm 54.5/\pm 54.2/\pm 53/\pm 55.7/\pm 52.8/\pm 53.5/\pm 51.1/\pm 51.2/\pm 52/\pm 51.4/\pm 48.9/\pm 48.2/\pm 44.7/\pm 38.8/\pm 33.6]_s$	2.082	31	36.04	31	5.568	31
	1/2	4	1.140	$[90_{32}]_s$	0.712	31	0.089	31	28.94	19

All generated optimum designs of anti-buckling behavior of 64 layered composite plates considering Puck failure criterion have been put together and presented in Table 6.17.

Table 6.17. All optimum designs of anti-buckling behavior

N_x (N/mm)	N_x/N_y	a/b	λ_{cb}	Stacking Sequence
1000	1/2	1	1.0867	$[\pm 45_2 / \mp 45 / \pm 45_2 / \mp 45_2 / \pm 45_3 / \mp 45_3 / \pm 45_3]_s$
		2	2.7972	$[\pm 88.8 / \pm 80.2 / \mp 78.2 / \mp 76.7 / \mp 80.5 / \mp 78.9 / \mp 72.6 / \mp 78.7 / \pm 79.2 / \pm 67.8 / \mp 83 / \mp 69.6 / \pm 88.5 / \mp 75.3 / \mp 60.4 / \pm 30.6]_s$
		4	11.4049	$[90_{32}]_s$
	1	1/2	1.2101	$[\pm 21.3 / \pm 23.4 / \pm 18.6 / \mp 20.5 / \pm 8.7 / \pm 26.5 / \pm 11.3 / \pm 17.8 / \mp 19.7 / \mp 14 / \mp 10.6 / \pm 3.5 / \mp 14.1 / \pm 34.2 / \pm 7.2 / \mp 42.4]_s$
		1	1.6301	$[\mp 45 / (\pm 45 / \mp 45_2)_2 / \pm 45 / \mp 45 / \pm 45_2 / \mp 45 / \pm 45_2 / \mp 45_2]_s$
		2	4.8486	$[\mp 71.7 / \pm 74 / \mp 70.4 / \mp 67.5 / \mp 71.1 / \mp 72.5 / \mp 70 / \pm 70.6 / \mp 70 / \mp 68.5 / \mp 69.4 / \mp 70.1 / \pm 67.2 / \pm 50.3 / \pm 74.9 / \mp 86]_s$
		4	20.5288	$[90_{32}]_s$
	2	1/2	1.3995	$[\pm 12.7 / \pm 8.5 / \pm 8.3 / \mp 11 / \pm 9.1 / \mp 14.6 / \pm 10.8 / \pm 11.2 / \mp 16.5 / \mp 13.3 / \pm 10 / \mp 16.2 / \pm 10.4 / \pm 10.3 / \pm 10.6 / \pm 7.7]_s$
		1	2.1735	$[\mp 45 / \pm 45 / \mp 45_2 / \pm 45 / \mp 45 / \pm 45_2 / \mp 45 / \pm 45 / \mp 45 / \pm 45_2 / \mp 45_2 / \pm 45_2]_s$
		2	7.5370	$[\pm 62.7 / \mp 61.7 / \pm 62.8 / \pm 61.8 / \mp 62.3 / \pm 62.5 / \pm 61.2 / \pm 62.5 / \mp 63.3 / \mp 62.3 / \mp 61 / \pm 60.2 / \pm 56.9 / \mp 70.1 / \pm 55.5 / \mp 89.9]_s$
		4	34.2147	$[90_{32}]_s$
	4	1/2	1.5095	$[0_{32}]_s$
		1	2.6082	$[\pm 45 / \mp 45 / \pm 45_2 / \mp 45 / \pm 45_3 / \mp 45_4 / \pm 45 / \mp 45_3]_s$
		2	10.0827	$[\mp 53.3 / \mp 53.4 / \pm 53.1 / \mp 52.9 / \pm 53.4 / \mp 53.4 / \mp 53.2 / \pm 53.3 / \mp 52.8_2 / \pm 53.4 / \mp 53.1 / \mp 52.7 / \pm 58.8 / \mp 51.1 / \pm 79.8]_s$
		4	51.3220	$[90_{32}]_s$

(Cont. on next page)

Table 6.17 (Cont.)

3000	1/2	4	3.8016	$[90_{32}]_s$
	1	2	1.6152	$[\mp 68.3/\pm 72/\pm 68.8/\mp 69.8/\pm 69.2/\pm 72.3/\mp 78/\pm 66.2/\pm 76.7/\mp 73.8/\pm 89.5/\mp 78.5/\mp 58.4/\mp 70.5/\pm 89.2/\pm 28]_s$
		4	6.8429	$[90_{32}]_s$
	2	2	2.5116	$[\pm 61.5/\mp 63.6/\mp 62.7/\pm 61.3/\pm 63.7/\mp 61.6/\mp 63.1/\pm 60.8/\mp 61.1/\pm 61.5/\mp 60.8/\pm 58/\mp 68/\pm 57.4/\pm 48.5/\pm 32]_s$
		4	11.4049	$[90_{32}]_s$
	4	2	3.3598	$[\pm 54.2/\mp 53.1/\pm 53.3/\mp 52.6/\pm 53.3/\mp 53.6/\pm 54.1/\pm 50.6/\pm 52/\mp 51.7/\mp 53.9/\pm 55/\mp 50.3/\mp 52.3/\pm 65.2/\pm 71.3]_s$
		4	17.1073	$[90_{32}]_s$
5000	1/2	4	2.2810	$[90_{32}]_s$
	1	4	4.1058	$[90_{32}]_s$
	2	2	1.5071	$[\pm 62.3/\pm 61.9/\mp 62.8/\mp 61.3/\mp 62.8/\pm 61.3/\mp 62.7/\pm 62/\pm 63.5/\pm 61.2/\mp 60.9/\mp 57.9/\pm 64.1/\mp 86/\pm 69.7/\mp 87.7]_s$
		4	6.8429	$[90_{32}]_s$
	4	2	2.0155	$[\mp 52.5/\mp 53.6/\mp 53.1/\pm 54.2/\pm 54.3/\pm 54.1/\pm 51.3/\mp 53.1_2/\pm 54.6/\pm 54.1/\mp 49.4/\pm 50.4/\pm 47.1/\mp 42.3/\pm 67.1]_s$
		4	10.2644	$[90_{32}]_s$
10000	1/2	4	1.1405	$[90_{32}]_s$
	1	4	2.0529	$[90_{32}]_s$
	2	4	3.4215	$[90_{32}]_s$
	4	4	5.1322	$[90_{32}]_s$

It can be seen from the table that 32 optimum designs of 64-layered carbon/epoxy composite plates have been obtained at the end of the process. Even though fiber orientations have been assumed continuous in the optimization study, discrete designs have been obtained. When the applied load N_x is increased, the number of optimum design withstanding to buckling and ply failure has been decreased at each design case. The most resistant plate designs have been obtained at the plate aspect ratios of 2 and 4. It can be observed that the critical buckling load factor values increase as load ratio and plate aspect ratio increase. It can be inferred from this situation that in-plane load in y-direction N_y and the width of the plate b are more effective parameters on plates in terms of buckling strength.

In addition to the investigation of optimum stacking sequence designs of composite plates in terms of the first ply failure using Puck fiber failure (FF) and inter-fiber failure mode B (IFFB), the investigation of optimum designs for only a specific loading case considering Puck inter-fiber failure mode C (IFFC) has also been studied.

Table 6.18. Inter-fiber failure efforts of optimum designs at N_x = 3000 N/mm loading for mode B ($f_{E(IFFB)}$) and mode C ($f_{E(IFFC)}$)

N_x/N_y	a/b	λ_{cb}	Stacking Sequence	LN_{cr}	$f_{E(IFFB)}$	LN_{cr}	$f_{E(IFFC)}$	θ_{fp}
1	1	0.5434	$[\pm 45/\mp 45/\pm 45/\mp 45/\pm 45/\mp 45_4/\pm 45_5/\mp 45/\pm 45]_s$	-	-	-	-	-
	2	1.6152	$[\mp 68.3/\pm 72/\pm 68.8/\mp 69.8/\pm 69.2/\pm 72.3/\mp 78/\pm 66.2/\pm 76.7/\mp 73.8/\pm 89.5/\mp 78.5/\mp 58.4/\mp 70.5/\pm 89.2/\pm 28]_s$	31	0.2609	31	0.4707	46.5
	4	6.8429	$[90_{32}]_s$	13	1.10^{-6}	1	1.25	53.9
	1/2	0.4032	$[\pm 17.9/\pm 25.7/\mp 23.4/\pm 19.4/\mp 11.1/\pm 5/\mp 20.1/\pm 19.3/\mp 7.4/\pm 24.9/\pm 20/\pm 21.9/\pm 19.7/\mp 35/\mp 19.3/\pm 48.8]_s$	-	-	-	-	-
2	1	0.7245	$[\mp 45_2/\pm 45_3/(\mp 45/\pm 45)_3/\mp 45_2/\pm 45_2/\mp 45]_s$	-	-	-	-	-
	2	2.5116	$[\pm 61.5/\mp 63.6/\mp 62.7/\pm 61.3/\pm 63.7/\mp 61.6/\mp 63.1/\pm 60.8/\mp 61.1/\pm 61.5/\mp 60.8/\pm 58/\mp 68/\pm 57.4/\pm 48.5/\pm 32]_s$	31	0.3693	31	0.4222	37.9
	4	11.405	$[90_{32}]_s$	29	2.10^{-8}	1	1.25	53.9
	1/2	0.4662	$[\mp 14.5/\pm 4.9/\pm 12.6/\pm 11.3/\pm 11/\pm 10.5/\pm 9.9/\pm 8.6/\pm 10/\pm 6.8/\pm 5.9/\pm 28.5/\mp 10.5/\pm 4/\pm 36.2/\mp 38.9]_s$	-	-	-	-	-
4	1	0.8694	$[\mp 45_2/(\pm 45/\mp 45)_2/(\mp 45/\pm 45)_2/\mp 45_5/\pm 45]_s$	-	-	-	-	-
	2	3.3598	$[\pm 54.2/\mp 53.1/\pm 53.3/\mp 52.6/\pm 53.3/\mp 53.6/\pm 54.1/\pm 50.6/\pm 52/\mp 51.7/\mp 53.9/\pm 55/\mp 50.3/\mp 52.3/\pm 65.2/\pm 71.3]_s$	25	0.4543	31	0.8987	47.9
	4	17.107	$[90_{32}]_s$	31	2.10^{-9}	21	1.25	53.9
	1/2	0.5032	$[0_{32}]_s$	-	-	-	-	-
1/2	1	0.3622	$[(\pm 45/\mp 45)_2/\mp 45/(\mp 45/\pm 45)_3/\mp 45_4/\pm 45]_s$	-	-	-	-	-
	2	0.9322	$[\mp 83.3/\mp 72.5/\mp 78.3/\mp 82.1/\mp 79.2/\pm 88.6/\mp 77.8/90_2/\mp 82.4/\mp 73.6/\pm 76.2/\pm 61.2/\pm 86.5/\mp 82.6/\pm 61.5/\pm 59.7]_s$	-	-	-	-	-
	4	3.8016	$[90_{32}]_s$	21	6.10^{-5}	3	1.2501	53.9
	1/2	0.3135	$[\pm 25.9/\mp 27.8_2/\mp 24.5/\pm 28.2/\pm 29.2/\pm 31.8/\pm 31.6/\pm 25.1/\mp 28.2/\mp 34.3/\pm 39.2/\pm 27/\pm 16.2/\mp 7.4/\pm 65.8]_s$	-	-	-	-	-

Table 6.18 represents the inter-fiber failure efforts of optimum designs at N_x = 3000 N/mm loading for mode B and C. Failure efforts, critical layer numbers and angle of fracture planes (θ_{fp}) of optimum designs according to IFF Mode C are given in the table. It is observed that some of the optimum designs according to IFF Mode B are not reliable or valid when IFF Mode C is considered and these cases are shown in grey color. The theory of mode C anticipates the fracture angles of inter-fiber planes with a good estimation, however mode B assumes that θ_{fp} = 0° (Knops 2008). It can be seen from the table that in consideration of Puck IFF Mode C, optimum designs of composite plates at plate aspect ratio of 4 have failed (because of $f_{E(IFFC)} > 1$), and the failure efforts and fracture plane angles of these design cases are the same, which are 1.25 and 53.9°, respectively. However, the optimum composite plate designs at aspect ratio of 2 have been found to be safe as in Puck IFF Mode B (due to $f_{E(IFFC)} < 1$). In these design cases, fractures are anticipated to occur at the same layers with angles such as 37.9°, 46.5° and 47.9° if the composite plates are critically loaded.

The performance of genetic algorithm for various design cases (N_x = 1000 N/mm loading, a/b = 1 plate aspect ratio, N_x/N_y = 1/2, 1, 2, 4 load ratios) depending on the best fitness values and generations is given in Figure 6.1.

The best and mean fitness values of objective functions for N_x = 1000 N/mm and a/b = 1 design cases at each generation can be seen in the figure. The best fitness value corresponds to critical buckling load factor (objective function) value and mean fitness value is the average of fitness values at each generation. The number of generations specifies the time when GA is to be stopped and is taken as 1000 for each design case. It is observed from the figures that the best fitness values improve more slowly in later generations and converge to the optimal point.

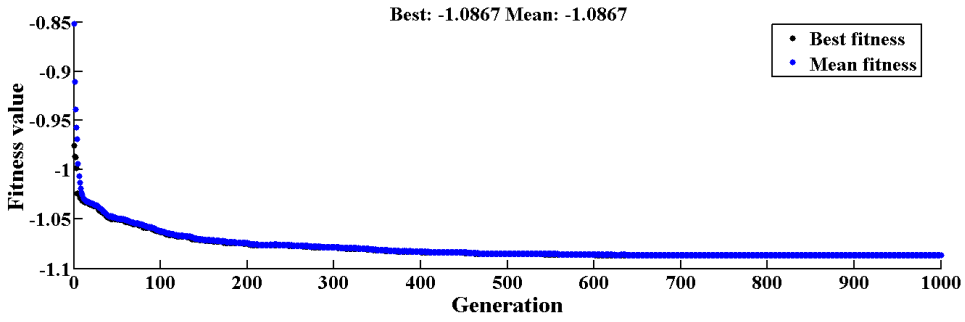

(a)

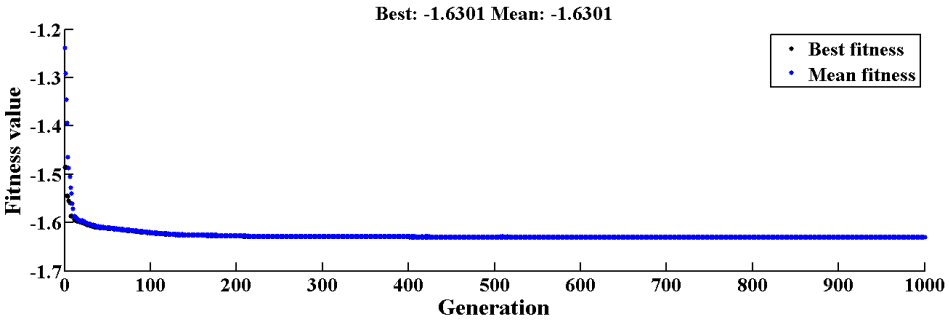

(b)

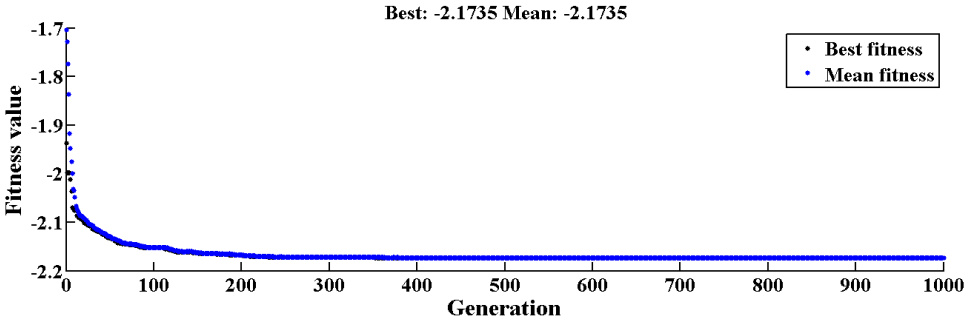

(c)

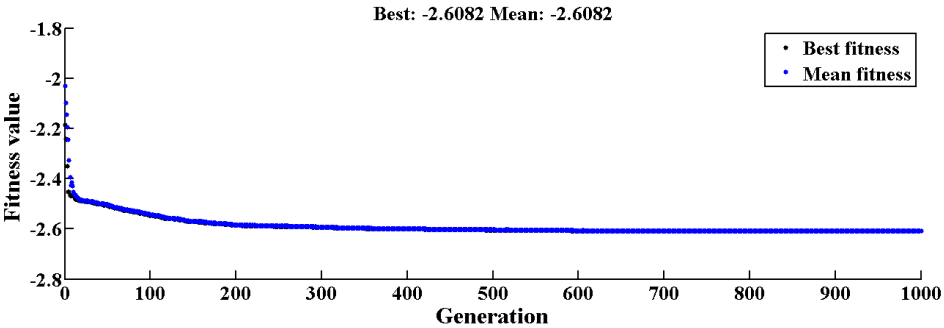

(d)

Figure 6.2. The best and mean values of the objective functions at each generation in GA for (a) $N_x/N_y = 1/2$, (b) $N_x/N_y = 1$, (c) $N_x/N_y = 2$, (d) $N_x/N_y = 4$

CHAPTER 7

CONCLUSION

In this thesis, the optimum designs of anti-buckling behavior of 64-layered carbon/epoxy composite plates subjected to in-plane compressive loading considering Puck failure criteria have been investigated. A stochastic search technique Genetic Algorithm (GA) has been considered as an optimization method. MATLAB Global Optimization and Symbolic Math Toolboxes have been used in optimization process. The critical buckling load factor is taken as objective function and fiber angles of the composite plates are taken as continuous design variables. The optimization has been performed for various loading cases (N_x / N_y = 1, 2, 4, 1/2) and aspect ratios ($a/b = 1$, 2, 4, 1/2) by maximizing critical buckling load factor for each case. N_x has been taken as 1000 N/mm, 3000 N/mm, 5000 N/mm and 10000 N/mm; the length of the plate a has been considered as 0.508 m. In order to increase the reliability of the optimization and achieve the best results, genetic algorithm has been run 50 times and stopped after 1000 evaluations at every turn.

First, verification of optimization algorithms of buckling load factor and Puck failure criterion has been performed using specific results given in previous studies in the literature.

Optimization of the composite plates which has specified design conditions has been carried out and eventually, at the end of the process, the optimum and bad plate designs in terms of buckling have been obtained. Following the optimization process, the optimum stacking sequence designs of composite plates have been checked layer by layer using Puck failure criteria in order to ensure that the layers are reliable in terms of the first ply failure. Then, totally, 32 optimum designs of 64-layered carbon/epoxy composite plates have been obtained. The findings of the process have revealed that the optimum design of a laminated composite depends on loading, loading ratio and plate aspect ratio as well. It has been observed that the critical buckling load factor values increase as load ratio and plate aspect ratio increase. It can be inferred from this situation that in-plane load in y-direction N_y and the width of the plate b are more effective parameters than the others on plates in terms of buckling strength.

The study was based upon the assumption of continuous fiber angles of stacking sequences, however both continuous and discrete stacking sequence designs of composite plates have been obtained. Some of the continuous stacking sequence designs have been converted into discrete designs and it has been concluded here that the continuous stacking sequence designs are more reliable in terms of buckling and ply failure resistance.

The optimization of 48-layered composite plates has been studied in order to be compared with 64-layered composite plates. It has been observed that the number of reliable composite plate designs and the values of critical buckling load factor decrease as compared to 64-layered designs.

A comparative study of Puck and Tsai-Wu failure criteria has been performed for critical optimum designs. The comparison has shown that further optimum designs resisting to buckling and the first ply failure have been obtained according to Puck failure criterion, however the number of optimum designs has decreased with consideration of Tsai-Wu failure criterion. This outcome has made the Puck failure criterion, as a design constraint, more advantageous than the other.

REFERENCES

Adali, S., Lene, F., Duvaut, G. and Chiaruttini, V., 2003, Optimization of laminated composites subject to uncertain buckling loads. *Composite Structures*. 62: p. 261-269.

Akbulut, M. and Sonmez, F. O., 2011, Design optimization of laminated composites using a new variant of simulated annealing. *Computers and Structures*. 89(17-18): p. 1712-1724.

Aymerich, F. and Serra, M., 2008, Optimization of laminate stacking sequence for maximum buckling load using the ant colony optimization (ACO) metaheuristic. *Composites: Part A*. 39: p. 262-272.

Erdal, O. and Sonmez, F. O., 2005, Optimum design of composite laminates for maximum buckling load capacity using simulated annealing. *Composite Structures*. 71: p. 45-52.

Gurdal, Zafer, Haftka, R. T. and Hajela, P., 1999, Design and Optimization of Laminated Composite Materials, *John Wiley & Sons, Inc.*

Haftka, R. T. and Le Riche, R., 1993, Optimization of laminate stacking sequence for buckling load maximization by genetic algorithm. *AIAA J*. 31(5): p. 951-956.

Irisarri, F. X., Bassir, D. H., Carrere, N. and Maire, J. F., 2009, Multiobjective stacking sequence optimization for laminated composite structures. *Composites Science and Technology*. 69: p. 983-990.

Karakaya, Ş. and Soykasap, Ö., 2009, Buckling optimization of laminated composite plates using genetic algorithm and generalized pattern search algorithm. *Struct Multidisc Optim*. 39: p. 477-486.

Kaw, Autar K., 2006, Mechanics of Composite Materials, *Taylor & Francis Group, LLC.*

Kim, C. W. and Lee, J. S., 2005, Optimal design of laminated composite plates for maximum buckling load using genetic algorithm. *Proceedings of the Institution of Mechanical Engineers, Part C: Journal of Mechanical Engineering Science*. 219: p. 869-878.

Knops, M., 2008, Analysis of Failure in Fiber Polymer Laminates, *Springer-Verlag Berlin Heidelberg New York.*

Le Riche, R. and Haftka, R. T., 1995, Improved Genetic Algorithm For Minimum Thickness Composite Laminate Design. *Composites Engineering*. 5(2): p. 143-161.

Liu, B., Haftka, R. T., Akgün, M. A. and Todoroki, A., 2000, Permutation genetic algorithm for stacking sequence design of composite laminates. *Comput. Methods Appl. Mech. Engrg*. 186: p. 357-372.

Lopez, R. H., Luersen, M. A. and Cursi, E. S., 2009, Optimization of laminated composites considering different failure criteria. *Composites: Part B*. 40: p. 731-740.

Mallick, P.K., 2007, Fiber-reinforced composites : materials, manufacturing, and design, *Taylor & Francis Group, LLC.*

Naik, G. N., Gopalakrishnan, S. and Ganguli, R., 2008, Design optimization of composites using genetic algorithms and failure mechanism based failure criterion. *Composite Structures*. 83: p. 354–367.

Pai, N., Kaw, A. and Weng, M., 2003, Optimization of laminate stacking sequence for failure load maximization using Tabu search. *Composites: Part B*. 34: p. 405-413.

Pelletier, J. L. and Vel, S. S., 2006, Multi-objective optimization of fiber reinforced composite laminates for strength, stiffness and minimal mass. *Computers and Structures*. 84: p. 2065–2080.

Puck, A. and Schürmann, H., 1998, Failure Analysis of FRP Laminates by means of Physically Based Phenomenological Models. *Composites Science and Technology*. 58: p. 1045-1067.

Rao, Singiresu S., 2009, Engineering optimization : theory and practice, *John Wiley & Sons, Inc.*

S.N.Sivanandam and S.N.Deepa, 2008, Introduction to Genetic Algorithms, *Springer-Verlag Berlin Heidelberg.*

Sebaey, T. A., Lopes, C. S., Blanco, N. and Costa, J., 2011, Ant Colony Optimization for dispersed laminated composite panels under biaxial loading. *Composite Structures*. 94(1): p. 31-36.

Soremekun, G., Gürdal, Z., Haftka, R. T. and Watson, L. T., 2001, Composite laminate design optimization by genetic algorithm with generalized elitist selection. *Computers and Structures*. 79: p. 131-143.

Soykasap, Ö. and Karakaya, Ş., 2007, Structural Optimization Of Laminated Composite Plates For Maximum Buckling Load Capacity Using Genetic Algorithm. *Key Engineering Materials*. 348-349: p. 725-728.

Spall, J. C., 2003, Introduction to stochastic search and optimization: estimation, simulation, and control, *John Wiley & Sons, Inc.*

Spallino, R. and Thierauf, G., 2000, Thermal buckling optimization of composite laminates by evolution strategies. *Computers and Structures*. 78: p. 691-697.

Topal, U. and Uzman, Ü., 2008, Thermal buckling load optimization of laminated composite plates. *Thin-Walled Structures*. 46: p. 667-675.

Topal, U. and Uzman, Ü., 2010, Multiobjective optimization of angle-ply laminated plates for maximum buckling load. *Finite Elements in Analysis and Design*. 46: p. 273-279.

Vinson, Jack R. and Sierakowski, Robert L., 2004, The Behavior of Structures Composed of Composite Materials, *Kluwer Academic Publishers.*

Walker, M., Reiss, T. and Adali, S., 1997, Optimal design of symmetrically laminated plates for minimum deflection and weight. *Composite Structures*. 39(3-4): p. 337-346.

Walker, M. and Smith, R. E., 2003, A technique for the multiobjective optimisation of laminated composite structures using genetic algorithms and finite element analysis. *Composite Structures*. 62: p. 123-128.

Xin-SheYang, 2010, Engineering optimization : an introduction with metaheuristic applications, *John Wiley & Sons, Inc.*

APPENDIX A

MATLAB COMPUTER PROGRAM

In this section, the computer program generating the objective functions (critical buckling load factors) in symbolic form is given.

```
clear all;
close all;
clc;
format short
theta_half = [sym('th(1)') -sym('th(1)') sym('th(2)') -sym('th(2)')...
   sym('th(3)') -sym('th(3)') sym('th(4)') -sym('th(4)')...
   sym('th(5)') -sym('th(5)') sym('th(6)') -sym('th(6)')...
   sym('th(7)') -sym('th(7)') sym('th(8)') -sym('th(8)') ...
   sym('th(9)') -sym('th(9)') sym('th(10)') -sym('th(10)')...
   sym('th(11)') -sym('th(11)') sym('th(12)') -sym('th(12)')...
   sym('th(13)') -sym('th(13)') sym('th(14)') -sym('th(14)')...
   sym('th(15)') -sym('th(15)') sym('th(16)') -sym('th(16)')];
theta = [theta_half fliplr(theta_half)];
Nplies = length(theta) %--> # plies
h_ply = 0.25*10^-3 %--> ply thickness[m]
E1 = 116.6*10^9; %[Pa]
E2 = 7.673*10^9; %[Pa]
G12 = 4.173*10^9; %[Pa]
NU12 = 0.270;
NU21 = (NU12*E2)/E1;
Q11 = E1/(1 - NU12*NU21);
Q12 = (NU21*E1)/(1 - NU12*NU21);
Q22 = E2/(1 - NU12*NU21);
Q66 = G12;
Q = [ Q11 Q12 0; Q12 Q22 0; 0 0 Q66];
```

```
%%% Calculation of D matrix %%%

t = Nplies * h_ply ;
for i = 1:(Nplies+1);
 h(i) = -(t/2-((i-1)*(t/Nplies)));
end

D=0;
 for i=1:Nplies
  a=theta(1,i);
  m=cos((a*pi)/180);
  n=sin((a*pi)/180);
  T = [ m^2 n^2 2*m*n; n^2 m^2 -2*m*n; -m*n m*n (m^2 - n^2)];
  Qbar = inv(T) * Q *(inv(T))' ;
  D = D + 1/3 * Qbar * (h(1,i+1)^3 - h(1,i)^3);
 end
 D;

 % In-Plane Loads %

 Nx = 5000000 %[N/m]
 Ny = 2500000 %[N/m]
 Nxy = 0;

 % Plate geometry %

 a=0.508; %[m]
 b=0.254; %[m]
 r=a/b % aspect ratio

%%%%%%%%%%%%%%%%%%%%%%%%%%%%%%%%%%%%%%%%%%%
```

```
m=1;n=1;
Nfbl = (pi^2)*(D(1,1)*(m^4) + 2*(D(1,2) + 2*D(3,3))*((r*m*n)^2)...
   + D(2,2)*((r*n)^4)); %failure buckling load
Nal = ((a*m)^2)*Nx + ((r*a*n)^2)*Ny; %applied load
Lamda_buckling11 = Nfbl/Nal;

m=1;n=2;
Nfbl = (pi^2)*(D(1,1)*(m^4) + 2*(D(1,2) + 2*D(3,3))*((r*m*n)^2)...
   + D(2,2)*((r*n)^4)); %failure buckling load
Nal = ((a*m)^2)*Nx + ((r*a*n)^2)*Ny; %applied load
Lamda_buckling12 = Nfbl/Nal;

m=2;n=1;
Nfbl = (pi^2)*(D(1,1)*(m^4) + 2*(D(1,2) + 2*D(3,3))*((r*m*n)^2)...
   + D(2,2)*((r*n)^4)); %failure buckling load
Nal = ((a*m)^2)*Nx + ((r*a*n)^2)*Ny; %applied load
Lamda_buckling21 = Nfbl/Nal;

m=2;n=2;
Nfbl = (pi^2)*(D(1,1)*(m^4) + 2*(D(1,2) + 2*D(3,3))*((r*m*n)^2)...
   + D(2,2)*((r*n)^4)); %failure buckling load
Nal = ((a*m)^2)*Nx + ((r*a*n)^2)*Ny; %applied load
Lamda_buckling22 = Nfbl/Nal;

%%%%%%%%%%%%%%%%%%%%%%%%%%%%%%%%%%%%%%%%%%%%%%

fid=fopen('buckling.m','w');
int=('function y = buckling(th)');
fprintf(fid,'%s\n',int);
lamdab11=char(Lamda_buckling11);
lamdab12=char(Lamda_buckling12);
lamdab21=char(Lamda_buckling21);
lamdab22=char(Lamda_buckling22);
fprintf(fid,'%s','y=-min([');
```

```
fprintf(fid,'%s%f',lamdab11);
fprintf(fid,'%s\n',',...');
fprintf(fid,'%s%f',lamdab12);
fprintf(fid,'%s\n',',...');
fprintf(fid,'%s%f',lamdab21);
fprintf(fid,'%s\n',',...');
fprintf(fid,'%s%f',lamdab22);
fprintf(fid,'%s\n',']);');
fclose(fid);

clear;
```